

# HEAF Modeling

## Modeling Approach and Analysis



Sandia  
National  
Laboratories



PRESENTED BY

Matt Hopkins, Ph.D., Paul Clem, Ph.D., Daniel Kotovsky, Ph.D. & Ken Armijo, Ph.D., Chris LaFleur, Ph.D.  
Electrical Science & Experiments, Conc. Solar Technologies, and Risk & Reliability Departments

July 24, 2019



Sandia National Laboratories is a multimission laboratory managed and operated by National Technology and Engineering Solutions of Sandia LLC, a wholly owned subsidiary of Honeywell International Inc. for the U.S. Department of Energy's National Nuclear Security Administration under contract DE-NA0003525.

# HEAF Modeling Approach Outline



- Background on physics modeling drivers
- Arc modeling plan
- Arc modeling approach
  - Lowke model
  - Small scale experiments
  - Particle characterization
- Multiphysics Arc Modeling Extension
  - Progress update
  - Next steps
- Target fragility and failure criteria
- Sandia National Labs models

# HEAF Modeling Needs



## CHARACTERIZATION OF TESTING AND EVENT EXPERIENCE FOR HIGH-ENERGY ARCING FAULT EVENTS

**EPRI** | ELECTRIC POWER  
RESEARCH INSTITUTE  
December 2017

If oxidation of aluminum is a minor effect, is there any difference between having copper and aluminum bus bars? If oxidation is minor, the energy released by oxidation is minor. However, the following other factors should be considered:

*Pressure-      Arc damage-      Metal splatter-*

Given these factors, it is difficult to fully quantify the differences between copper and aluminum bus bars and the ultimate effect on the severity of a HEAF event. **More research could better determine how these effects contribute to overall damage and especially fire starting in cables in switchgear and external equipment.** Basic tests of arcing and oxidation could address fundamental questions, such as:

- How much of the aluminum oxidizes for different event scenarios (different bus arrangements, currents, and durations)?
- How different is aluminum versus copper for comparable scenarios?
- How do different bus arrangements (vertical, horizontal, angled, terminated, and so on) affect melting and vaporization of aluminum?
- How do enclosure geometry and venting affect oxidation and energy release?

EPRI Product Id: 3002011922

<https://www.epri.com/#/pages/product/000000003002011922/?lang=en-US>

# Goal: Provide improved predictive capability of HEAF incident energy leveraging Sandia air plasma models



## Photovoltaics

**Bakersfield CA, April 5 2009**

“... the ground-fault protection device was unable to interrupt the current, **allowing arc faults to be formed**, spreading sparks to surrounding materials, **causing ignition.**”

-- Commercial Roof-Mounted Photovoltaic System Installation Best Practice Review and All Hazard Assessment, The Fire Protection Research Foundation, Feb. 2014



## Nuclear Energy

**San Onofre Nuclear Generating Station, Feb. 3 2001**

“There was a **failure of the main contacts** of a 25 year old 4.16 kV breaker to close fully, **causing a HEAF event... the fire persisted for three hours** until water was applied.”

-- Brown et al., SAND2008-4820, High energy arcing fault fires in switchgear equipment, a literature review

# Provide Improved Prediction of HEAF Incident Energy



## DIRECT CURRENT ARC-FLASH HAZARDS OF SOLAR PHOTOVOLTAIC SYSTEMS

**EPRI** | ELECTRIC POWER RESEARCH INSTITUTE | October 2018

Figure 7 shows the arc-flash incident energies calculated for a 1-MWdc nameplate capacity PV system using four different methods and an experimentally measured value [17]. The experiments were performed on a utility-owned ground-mount photovoltaic plant with a 1-MWdc nameplate capacity located at Sturbridge, Massachusetts. The arc-flash experiments were performed in the following PV equipment: a combiner box, an inverter, and a calibration box (a 20 x 20 x 20-inch metal cube) at 250 kW, 500 kW, and 1,000 kW of array capacity. The behavior of the arc, including current, voltage, and power was evaluated for different equipment conditions and different PV array connections.

Accurate arc models needed to avoid overprediction of damage

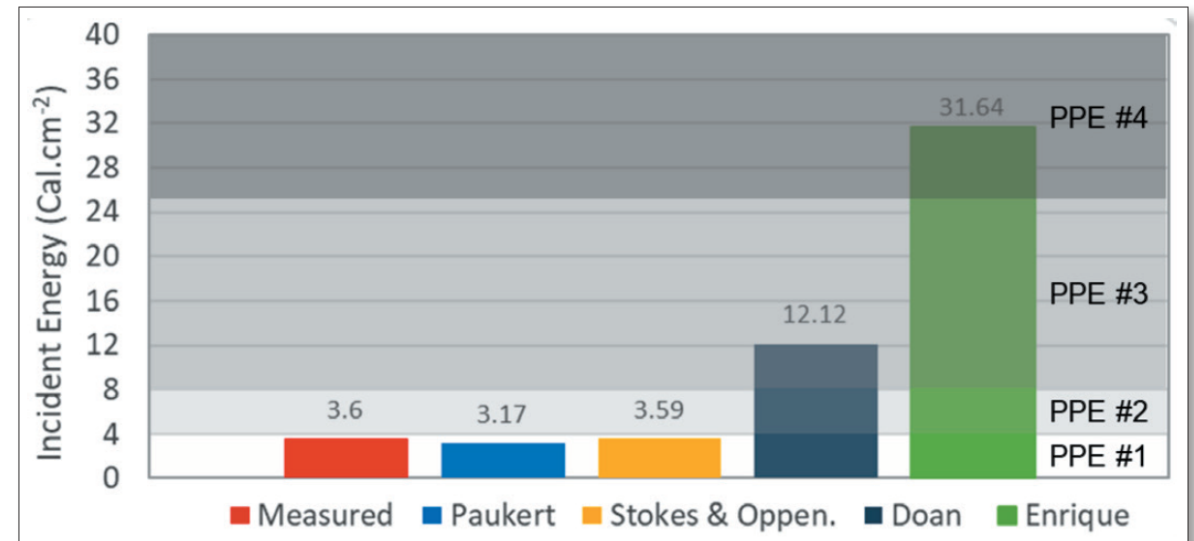


Figure 7 – Bar chart of incident energy measured and calculated using simplified models for a 1-MW PV system in inverter level and respective PPE categories according to NFPA 70E-2018

EPRI Product Id: 3002014641

<https://www.epri.com/#/pages/product/000000003002014641/?lang=en-US>

Aim: arc physical model, where DC current and electrode gap → radiation, convective and thermal energy transport

# Opportunities in AC Arc Modeling



## “Tools for the Simulation of the Effects of the Internal Arc in Transmission and Distribution Switchgear”

### Working Group A3.24, December 2014

#### 4.3.2 Arc and gas models in CFD, and other enhancements

The programming interface allows the implementation of user-defined algorithms. In the simplest approach, the arc is modeled by an energy input, which is homogeneously distributed in the arc compartment volume, using the thermal transfer coefficient  $k_p$  described in Chapter 2.

In a more detailed approach [Besnard2009], the arc heating power is confined to a small number of finite volumes in the vicinity of the arc initiation point. In order to balance the temperature rise in these finite volumes, a model of the radiation process is needed. As a result, the temperatures in the vicinity of the arc initiation point reach high values (11000 K in air typically), whereas the arc compartment still includes cold gas regions, as do the other compartments. This accounts for the high temperature gradients existing during the internal arc event, leading to high density gradients.

The most complete approaches, where the arc would be modeled using physical equations describing the arc roots, the arc plasma column, the effect of electro-magnetic fields on the motion of the arc, the transfer of energy from the arc plasma to the surrounding gas etc. have never been applied to internal arc to our knowledge.

Aim: arc physical model, where AC current and electrode gap → radiation, convective and thermal energy transport

602

Tools for the Simulation of the Effects of the Internal Arc in Transmission and Distribution Switchgear

Working Group A3.24

December 2014

CIGRE

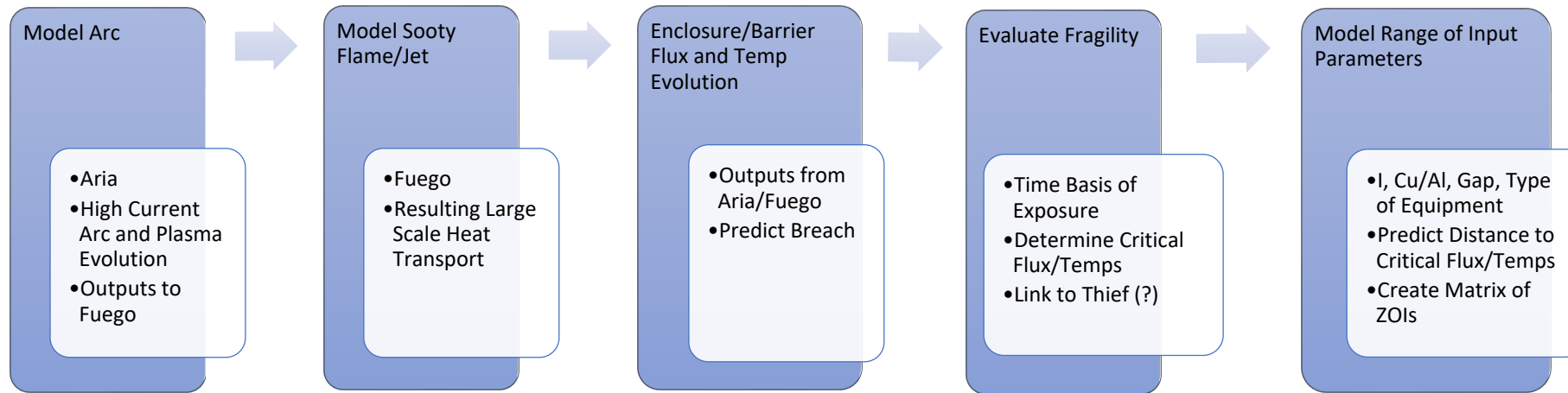
TOOLS FOR THE SIMULATION OF THE EFFECTS OF THE INTERNAL ARC IN TRANSMISSION AND DISTRIBUTION SWITCHGEAR

WG A3.24

Members

N. Uzelaç, **Convenor** (US) M. Glinkowski, **Secretary** (US), L. del Rio (ES), M. Kriegel, **Former Convenor** (CH), J. Douchin (FR), E. Dullni (DE), S. Feitoza Costa (BR), E. Fjeld (NO), H-K. Kim (KR), J. Lopez-Roldan (AU), R. Pater (CA), G. Pietsch (DE), T. Reiher (DE), G. Schoonenberg (NL), S. Singh (DE), R. Smeets (NL), T. Uchii (JP), L. Van der Sluis (NL), P. Vinson (FR), D. Yoshida (JP)

# Arc Modeling Plan Overview



Vision: Non-conservative estimate of credible energy release scenarios and respective zones of influence for range of appropriate equipment at NPP

Goal to develop model and resulting look-up table for:

- Arc plasma emission as a function of current and gap
- Incident energy as a function of current, breach geometry, and electrode material

Measurements for validation

- Incident energy (slug/plate calorimeters)
- Thermal field (calorimeters, calibrated IR cameras)
- Radiated power (black ASTM calorimeters)
- Fragility samples (cables, secondary equipment enclosures, others as needed)
- Particle characterization (oxidation and morphology)

# Modeling Plan



- Accurate validated predictive modeling is an iterative process
- Basic physics of the arc must be characterized first in Aria. Start with simple model of arc only and determine governing equations, make predictions, and compare to experimental measurements.
  - Arc temperature, radius, radiative and heat transfer characteristics of emitted energy, and mass loss rate of conductors will be first parameters modeled
- Complexity will be added in layers
  - Effects of magnetic forces, buoyancy, and orientation of conductors
- Each output parameter of the model will tie directly into the failure characterization of target equipment and will be measured and compared to small and large scale experimental data
- Model is not intended to be used by licensees, it is tool to aid joint NRC/EPRI Working group to make decisions on realistic ZOIs for a wider range of HEAF scenarios

# Output of the Modeling Effort



- Output will be spatial characterization of emitted energy that, when combined with failure criteria for key targets, can be used by HEAF working Group to determine zones of influence
- Modeling will provide a tool for characterizing the HEAF hazard from a variety of scenarios
- Physics model will provide more realistic predictive capability and reduce need for costly experiments
- Parameters that are critical for determining if failure criteria for targets are being measured in full-scale experiments
- Model validation and quantification of total Joule heating ( $I^2R_{\text{arc}}\Delta t$ ) is measured by:
  - Arc voltage, current, and resistance
  - Radiated power (ASTM black Cu calorimeters), Electrode temperature (calibrated IR cameras)
  - Arc temperature (UV-visible-NIR spectroscopy)
  - Arc dynamics (high speed cameras)

# Arc Modeling Approach



Physical arc-fault energy models may be developed using prior literature and knowledge of:

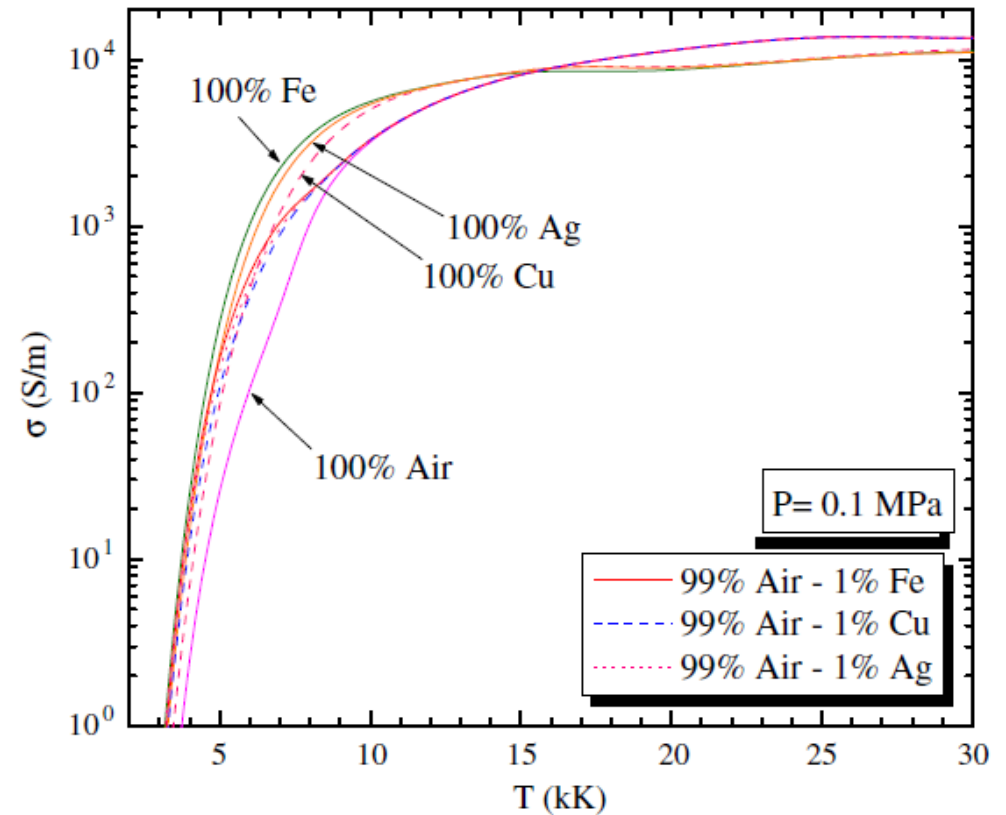
- Electrode gap
- Electrode metal (Cu, Al, ...)
- Input current (100 A to 100 kA)
- Conductivity of ambient (air, air + Al, air + Cu)
- Thermal properties of ambient gas



KEMA HEAF test switchgear  
Al bus bars, 11.5 cm gap

Influence of metallic vapours on the properties of air thermal plasmas

Y Cressault *et al* 2008 *Plasma Sources Sci. Technol.* 17 035016



Influence of metallic vapours on the electrical conductivity.

# Arc Modeling Approach



Physical arc-fault energy models may be developed using prior literature and knowledge of:

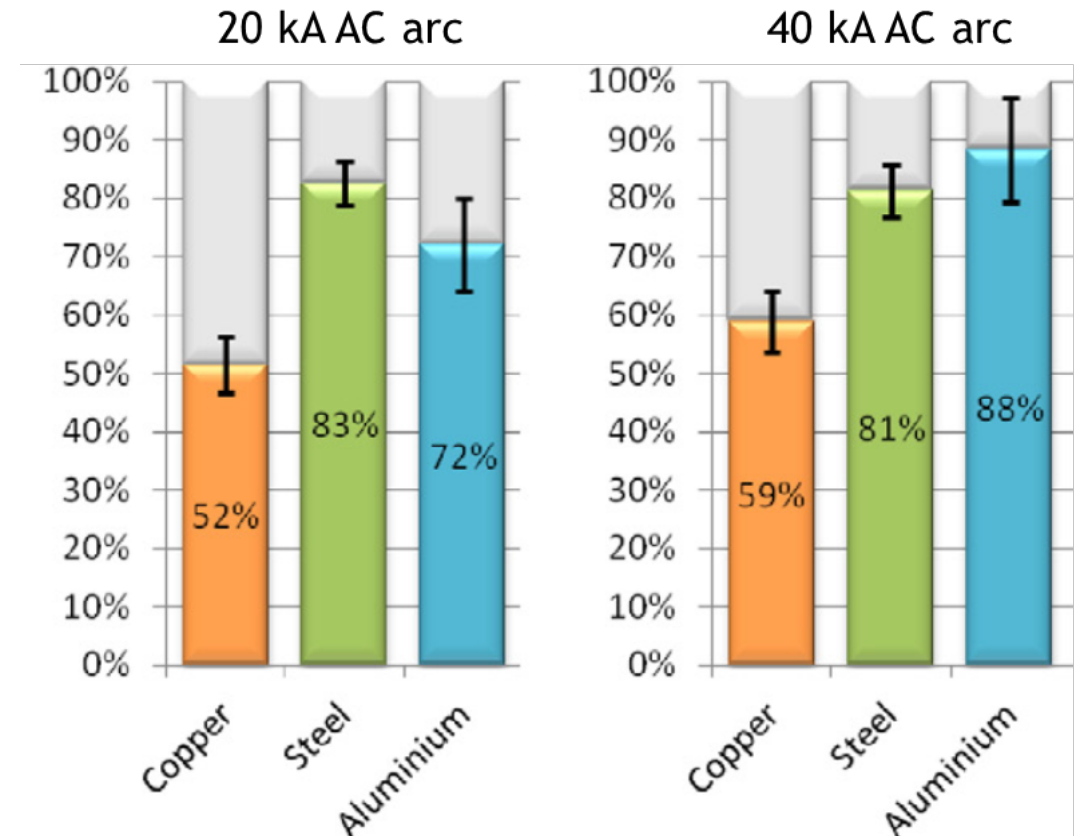
- Electrode gap
- Electrode metal (Cu, Al, ...)
- Input current (100 A to 100 kA)
- Conductivity of ambient (air, air + Al, air + Cu)
- Thermal properties of ambient gas



KEMA HEAF test switchgear  
Al bus bars, 11.5 cm gap

Radiation of long and high power arcs

Y. Cressault et al. J. Phys. D: Appl. Phys. 48 415201 (2015)



Proportion of radiative energy (with SD) relative to the total arc energy.

# Arc Modeling Approach



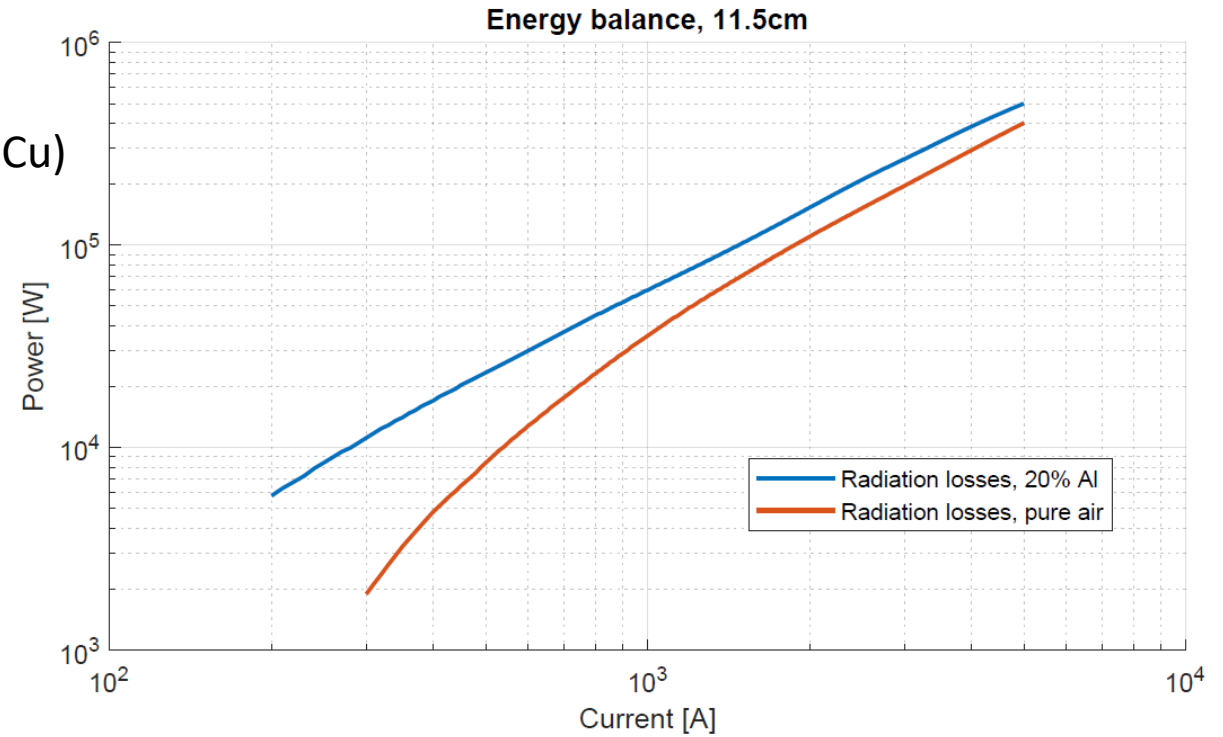
Physical arc-fault energy models:

- Electrode gap
- Electrode metal (Cu, Al, ...)
- Input current (100 A to 100 kA)
- Conductivity of ambient (air, air + Al, air + Cu)
- Thermal properties of ambient gas



KEMA HEAF test switchgear  
Al bus bars, 11.5 cm gap

Prediction of arc voltage, radius, temperature and power



Basis: JJ Lowke "Simple theory of free-burning arcs,"  
J. Phys D 12, (1979)

# Lowke Model: Isothermal Arc Model



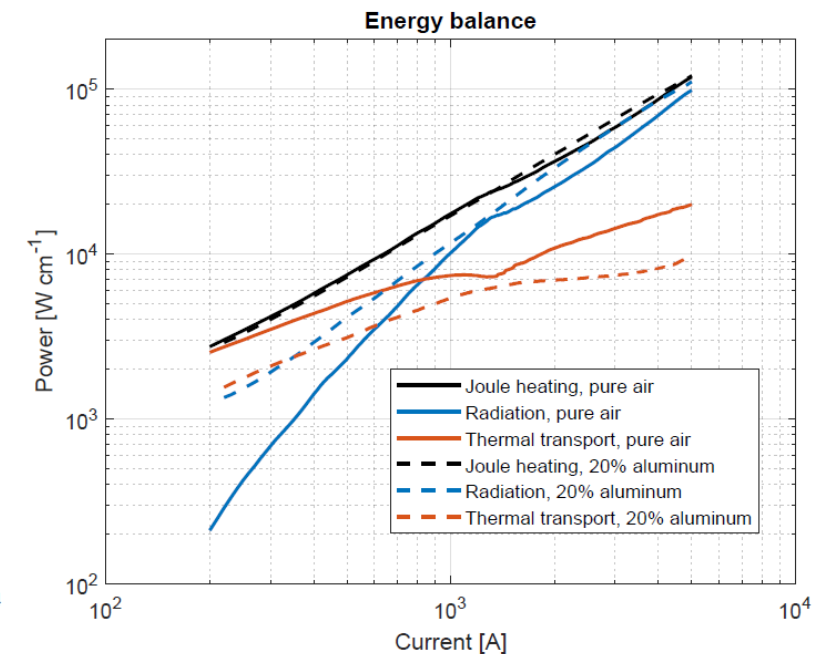
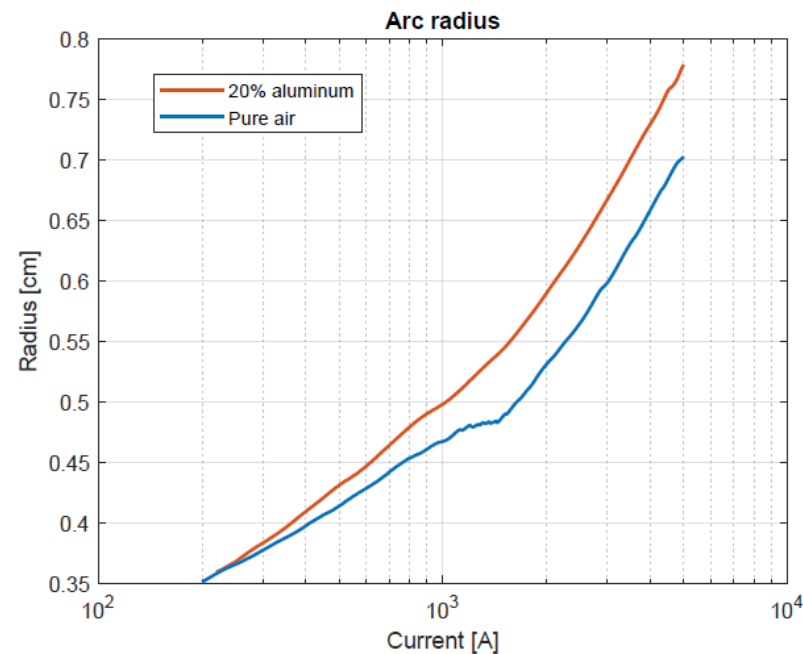
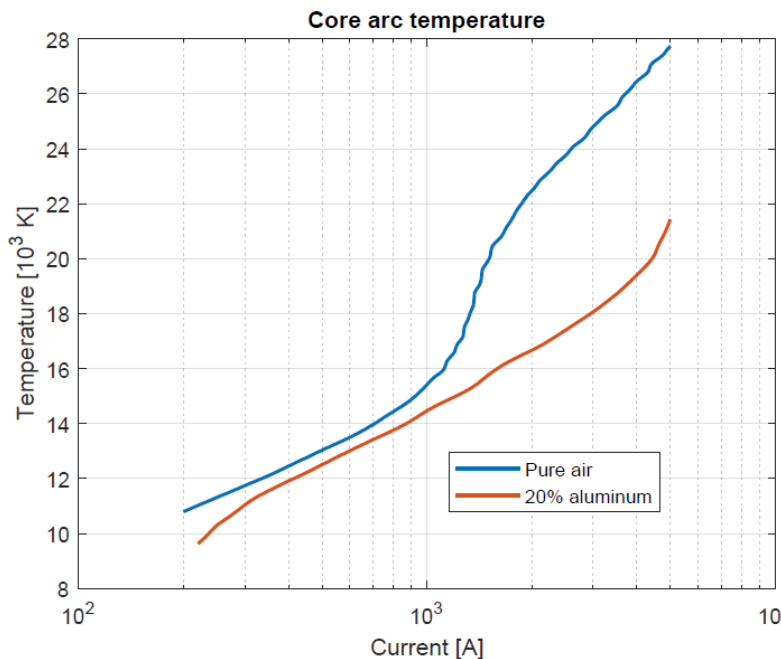
## Assumptions:

- Arc is in equilibrium and isothermal vs. radius
- Electrode thermal effects are neglected
- Air conductivity, air+Al conductivity calculated

Reference: JJ Lowke “Simple theory of free-burning arcs,”  
J. Phys D 12, (1979)

<https://iopscience.iop.org/article/10.1088/0022-3727/12/11/016/meta>

Total energy output (source term):  
radiation + convection + conduction

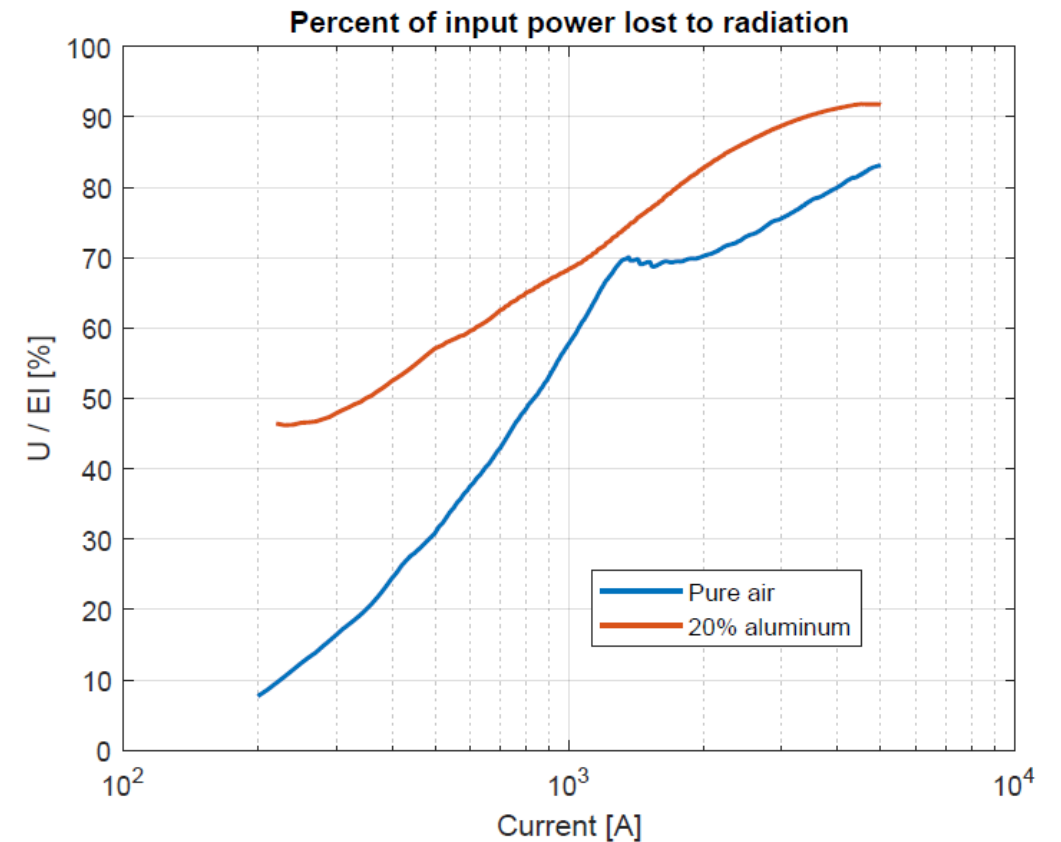
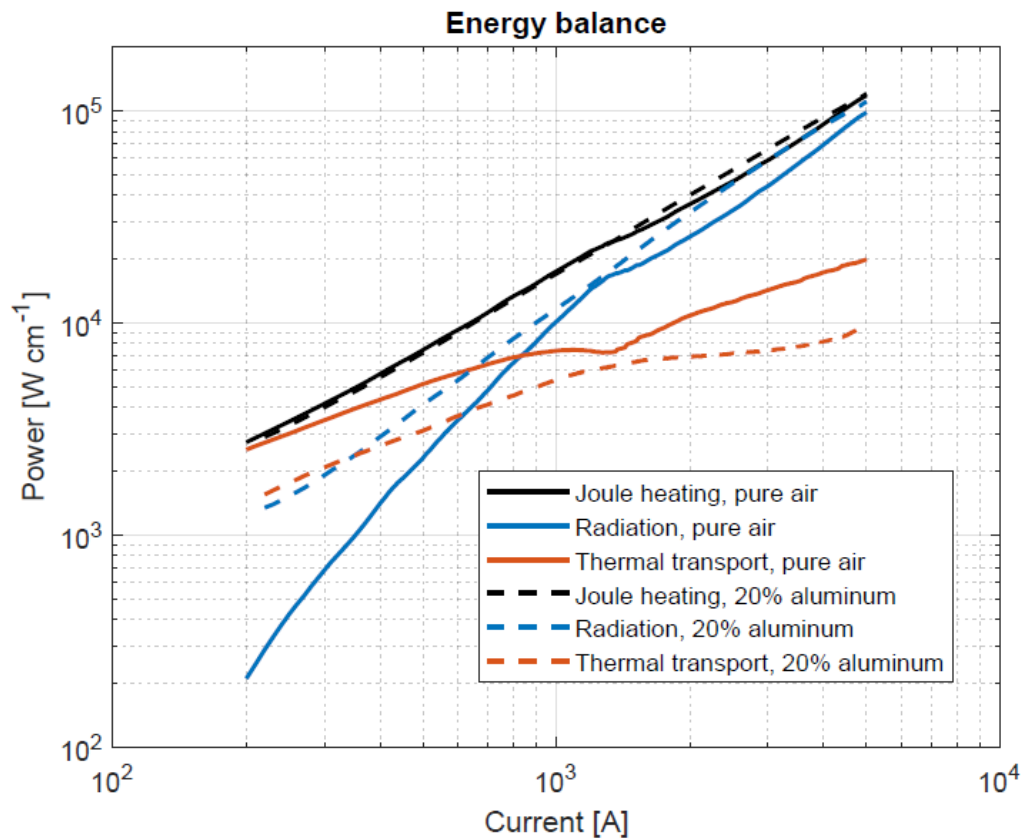


# Lowke Model: Isothermal Arc Model Predictions



## Predictions:

- HEAF arc energy is dominated by radiation at  $> 1$  kA
- Presence of electrode vapor (Al or Cu) increases radiation



# Small Scale Experiments for Modeling Validation



Experimental testbeds have been developed for two capabilities:

1. A capacitive discharge system for which a charge voltage of 1.5-11 kV, produces a stored energy 1-50 kJ, to support short duration arcs (100 ms) at high current (1 kA - 160 kA).
2. A long-duration (1-120 s), arc-triggering constant current source, which uses a 100 A – 1 kA constant current supply

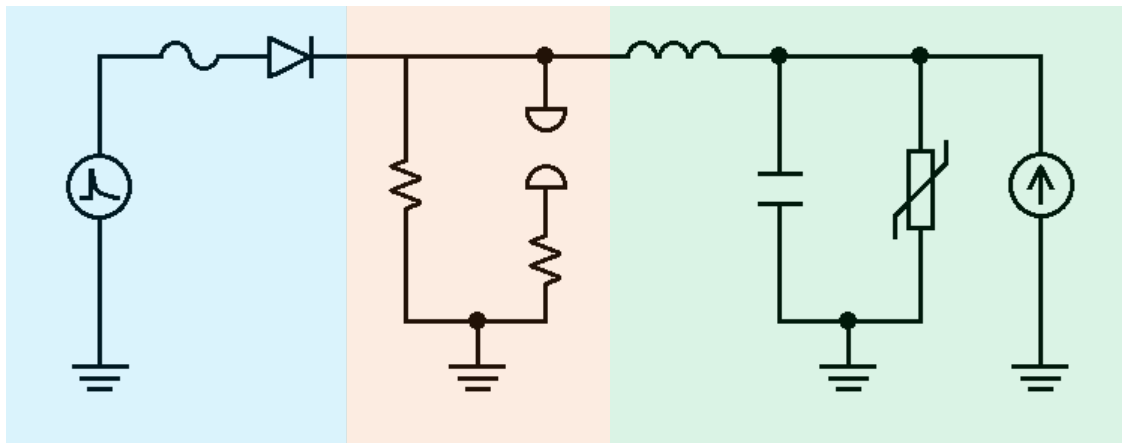
Reproducible 30 s arc tests with Al, Cu, Fe & C electrodes have been performed at constant current

## Constant Current Source Arc-Generator Circuit Diagram

Impulse generator  
with reverse current  
protection

Test gap with  
voltage and  
current  
diagnostics

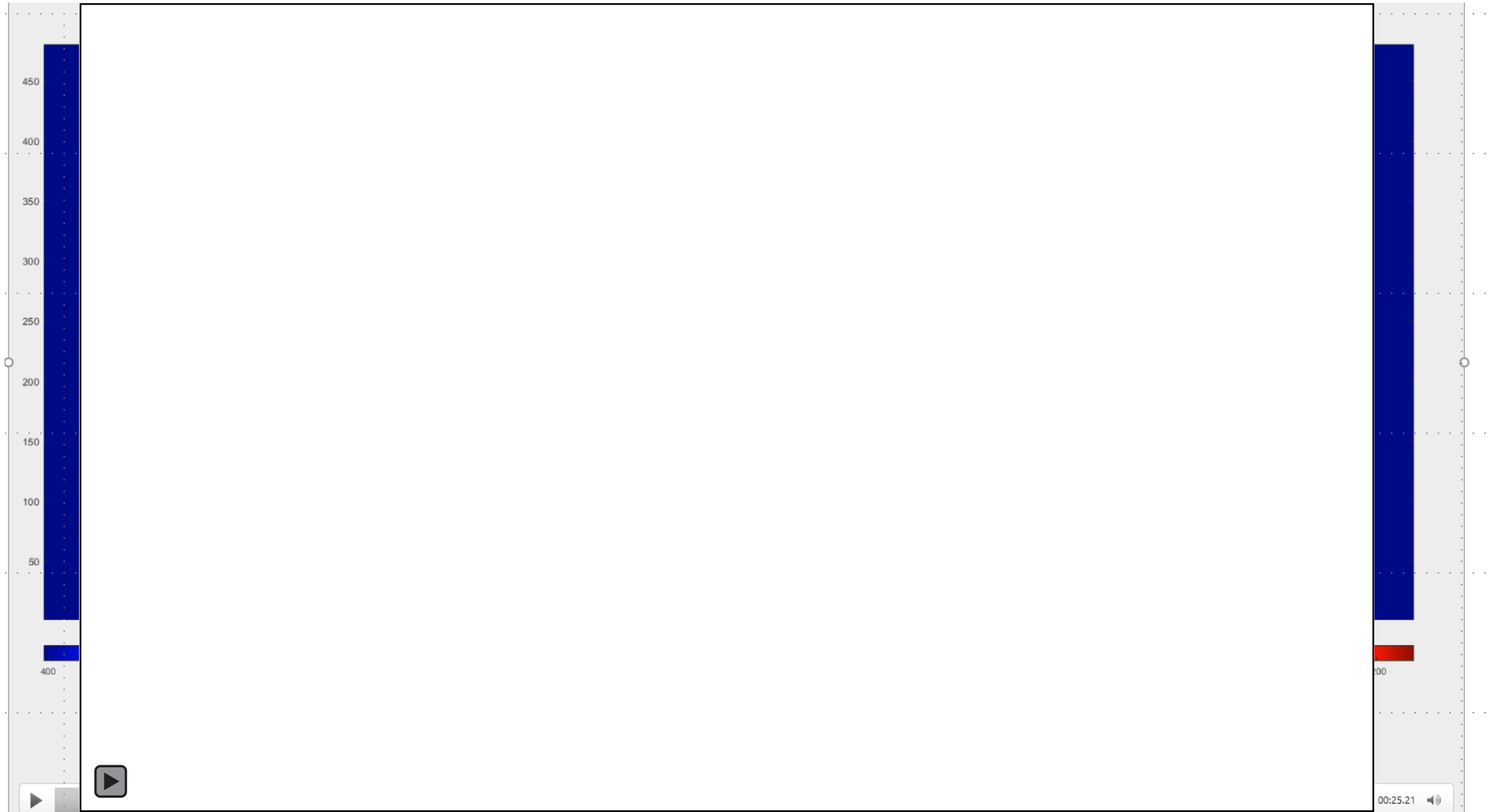
Current source with line  
filter and transient  
voltage suppression



### Measurements include:

- Arc voltage, arc current, radiated power, thermal power
- Arc temperature (spectroscopy), IR cameras (calibrated to 3000K)

# Lowke Model: Initial DC Experiments (5 second arcs)



# Lowke Model: Initial DC Experiments (5 second arcs)



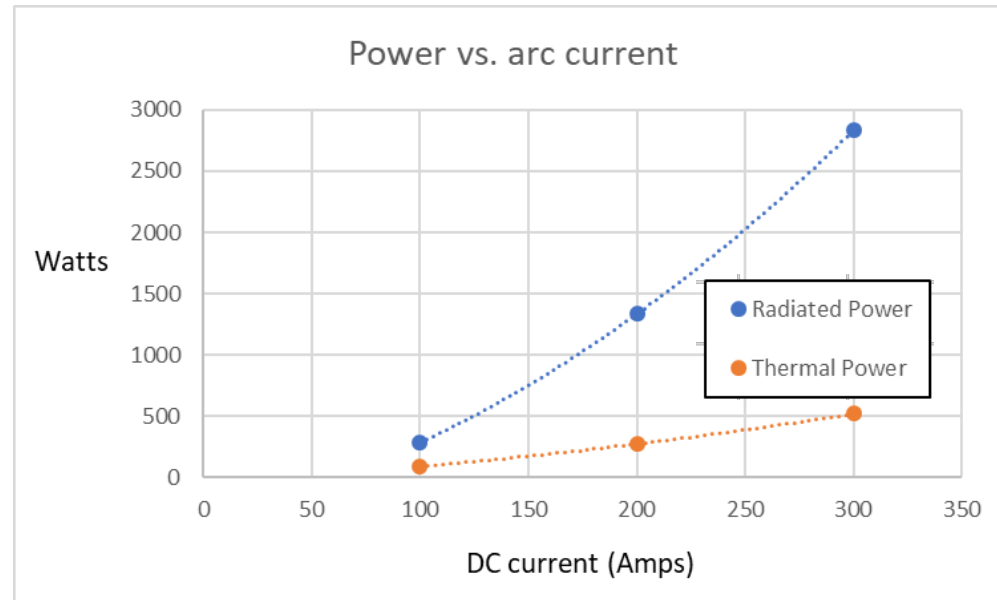
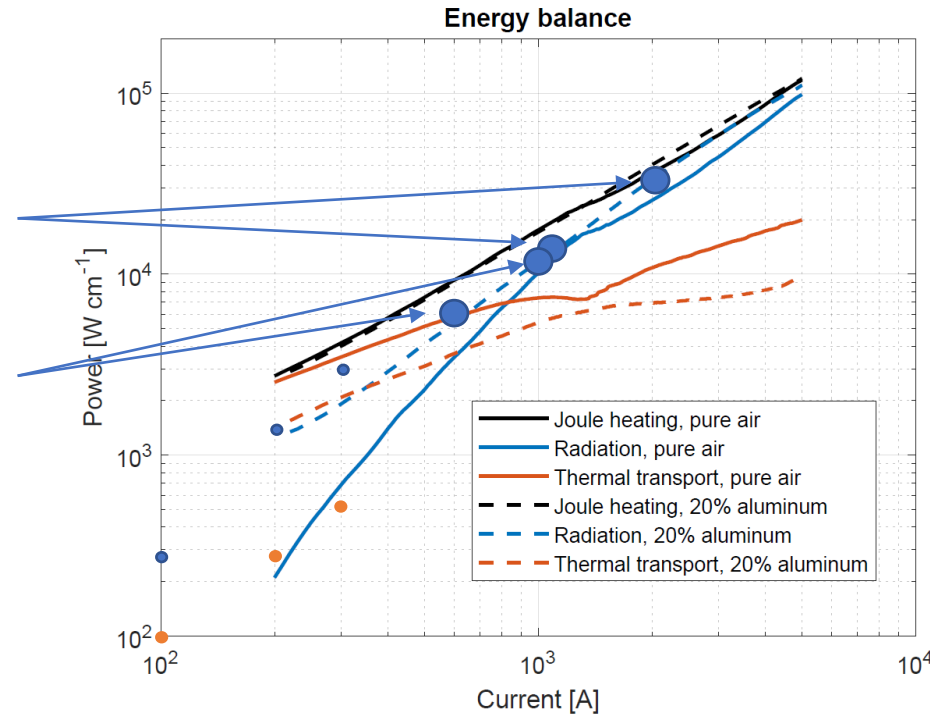
# Lowke Model: Initial DC Experiments



- Capability established for DC arc measurements at 50A to 500A to compare to arc models.  
Radiation power measured agrees to model within 10-30%
- Evaluating vertical, horizontal & parallel arc between Al and Cu electrodes during summer 2019

KEMA testing  
Aug-Sep 2019

Sandia testing  
July-Aug 2019



What we measure for model validation and quantification of total Joule heating ( $I^2 R_{\text{arc}} \Delta t$ ):

- $V_{\text{arc}}, I_{\text{arc}}$  ( $\rightarrow R_{\text{arc}}(t)$ )
- Radiated power (ASTM black Cu calorimeters), Electrode temperature (calibrated IR cameras)
- Arc temperature (UV-visible-NIR spectroscopy)
- Arc dynamics (high speed cameras)

# Prior Small Scale Bus Bar Experiments

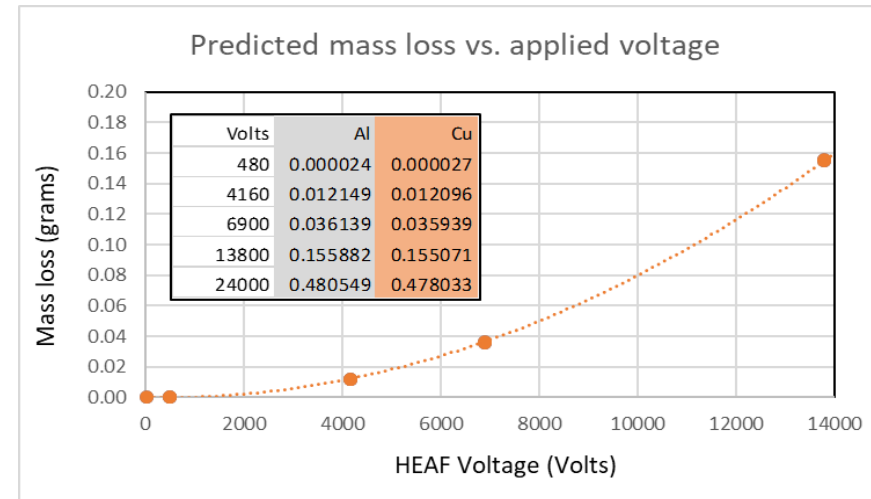


- Variable voltage: 480 V, 4160V, 6900V, 10 kV, 100 ms arcs applied to copper vs. aluminum bus bars
- Bus bars were scaled to similar current density to KEMA HEAF testing

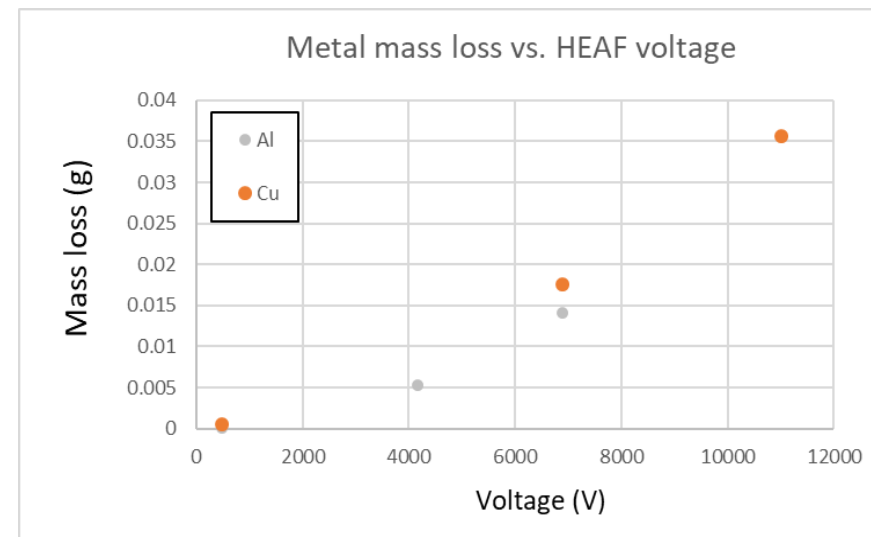


Table 3-1. Primary small-scale test matrix

Test no.	Sub no.	Test Month	Charge voltage [V]	Current-limiting resistance [ $\Omega$ ]	Arc duration [msec]	Estimated peak current [A]	Estimated scale current [kA]	Gap size [mm]	Bus bar material
1	A	July	583	9.9	24.2	50	1.6	5	Al
	B	August	643	9.9	21.4	55.4	2.4	5	Al
	C	August	599	10	22.5	55.3	2.2	5	Al
	D	August	631	10	24.2	51.3	2.2	5	Al
2	A	July	571	9.9	22.9	49	1.6	5	Cu
3	A	July	543	5.1	13.6	91	2.9	5	Al
	B	August	590	5	12	97.1	3.9	5	Al
	C	August	587	5	13.3	98.2	3.7	5	Al
4	A	July	543	5.1	13.5	91	2.9	5	Cu
5	A	July	6787	9.9	35.3	690	22	5	Al
	B	August	6876	10	33.7	663	23	5	Al
	C	August	6835	10	34.6	663	22	5	Al
6	A	July	6781	10	41	680	21	5	Cu
7	A	July	6832	5.1	19.4	1300	42	5	Al
	B	July	6742	5.1	21.3	1300	42	5	Al
	C	August	6826	5	19	1280	42	5	Al
	D	August	6870	5	18.3	1290	43	5	Al
9	A	July	6757	5.1	23.8	1300	42	5	Cu
10	A	July	6778	19.6	81.2	350	11	5	Al
	B	August	6793	19.7	73.3	339	11	5	Al
	C	August	6907	19.7	74.5	350	11	5	Al
11	A	July	6794	9.9	29.6	690	22	10	Al
12	A	July	6838	9.9	33.8	690	22	10	Cu
13	A	July	6762	5.1	21.2	1300	42	10	Al
14	A	July	6900	5.1	23.6	1300	42	10	Cu
15	A	July	4098	9.9	39.2	410	13	5	Al
	B	August	4129	10	29.7	396	14	5	Al
	C	August	4140	10	30.9	398	14	5	Al
16	A	July	4065	5.1	14.5	800	25	5	Al
	B	August	4222	5	18.1	792	26	5	Al
	C	August	4156	5	17	777	27	5	Al
17	A	July	9861	32.3	127.9	310	9.7	5	Al
	B	August	9197	31.2	111	282	9.7	5	Al
	C	August	9175	31.2	120	285	9.4	5	Al
18	A	July	9944	33	132	310	9.7	5	Cu
19	A	July	9893	33	132	310	9.7	10	Al
20	A	July	9984	33	132	310	9.8	10	Cu



Predicted  $V^2/R$  scaling of mass loss vs. HEAF voltage: note Al & Cu data overlap.



Measured  $V^2/R$  scaling of mass loss vs. HEAF voltage.

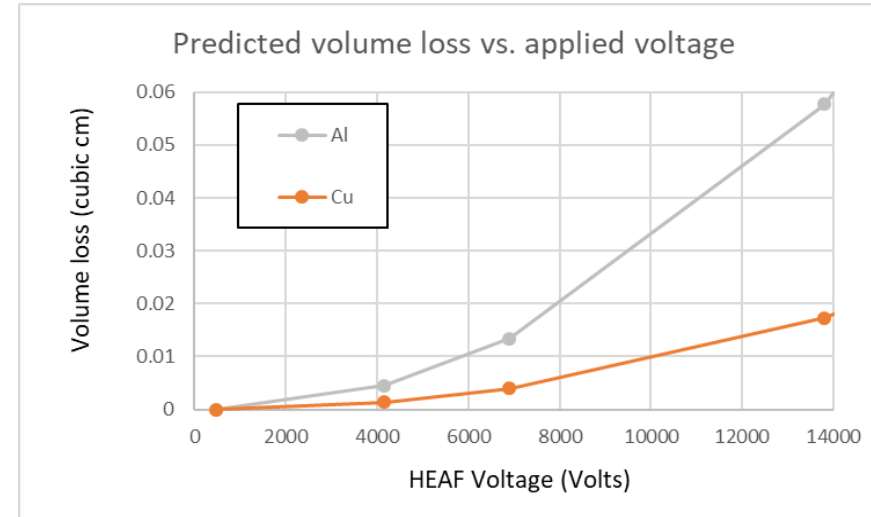
# Prior Small Scale Bus Bar Experiments



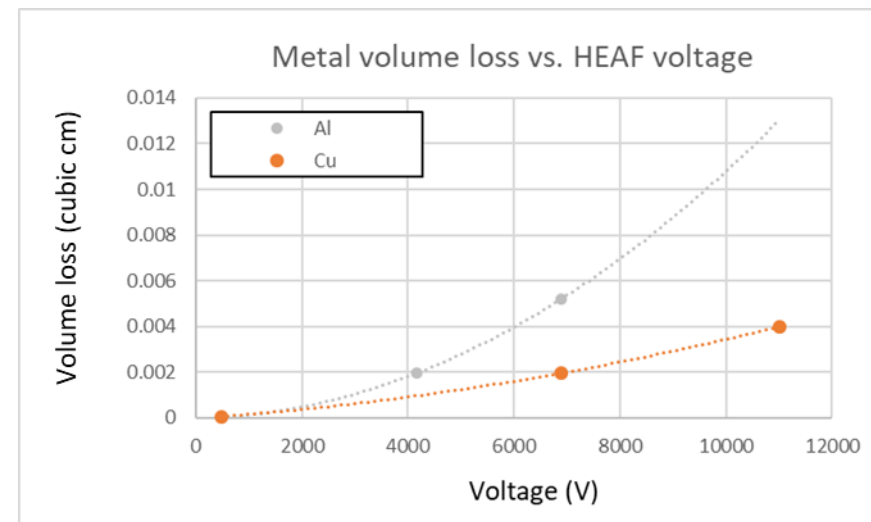
- Variable voltage: 480 V, 4160V, 6900V, 13.8 kV, 100 ms arcs applied to copper vs. aluminum bus bars
- Bus bars were scaled to similar current density to KEMA HEAF testing

Table 3-1. Primary small-scale test matrix

Test no.	Sub no.	Test Month	Charge voltage [V]	Current-limiting resistance [ $\Omega$ ]	Arc duration [msec]	Estimated peak current [A]	Estimated scale current [kA]	Gap size [mm]	Bus bar material
1	A	July	583	9.9	24.2	50	1.6	5	Al
	B	August	643	9.9	21.4	55.4	2.4	5	Al
	C	August	599	10	22.5	55.3	2.2	5	Al
	D	August	631	10	24.2	51.3	2.2	5	Al
2	A	July	571	9.9	22.9	49	1.6	5	Cu
3	A	July	543	5.1	13.6	91	2.9	5	Al
	B	August	590	5	12	97.1	3.9	5	Al
	C	August	587	5	13.3	98.2	3.7	5	Al
4	A	July	543	5.1	13.5	91	2.9	5	Cu
5	A	July	6787	9.9	35.3	690	22	5	Al
	B	August	6876	10	33.7	663	23	5	Al
	C	August	6835	10	34.6	663	22	5	Al
6	A	July	6781	10	41	680	21	5	Cu
7	A	July	6832	5.1	19.4	1300	42	5	Al
	B	July	6742	5.1	21.3	1300	42	5	Al
	C	August	6826	5	19	1280	42	5	Al
	D	August	6870	5	18.3	1290	43	5	Al
9	A	July	6757	5.1	23.8	1300	42	5	Cu
10	A	July	6778	19.6	81.2	350	11	5	Al
	B	August	6793	19.7	73.3	339	11	5	Al
	C	August	6907	19.7	74.5	350	11	5	Al
11	A	July	6794	9.9	29.6	690	22	10	Al
12	A	July	6838	9.9	33.8	690	22	10	Cu
13	A	July	6762	5.1	21.2	1300	42	10	Al
14	A	July	6900	5.1	23.6	1300	42	10	Cu
15	A	July	4098	9.9	39.2	410	13	5	Al
	B	August	4129	10	29.7	396	14	5	Al
	C	August	4140	10	30.9	398	14	5	Al
16	A	July	4065	5.1	14.5	800	25	5	Al
	B	August	4222	5	18.1	792	26	5	Al
	C	August	4156	5	17	777	27	5	Al
17	A	July	9861	32.3	127.9	310	9.7	5	Al
	B	August	9197	31.2	111	282	9.7	5	Al
	C	August	9175	31.2	120	285	9.4	5	Al
18	A	July	9944	33	132	310	9.7	5	Cu
19	A	July	9893	33	132	310	9.7	10	Al
20	A	July	9984	33	132	310	9.8	10	Cu



Predicted  $V^2/R$  scaling of volume loss vs. HEAF voltage: note Al & Cu data overlap.

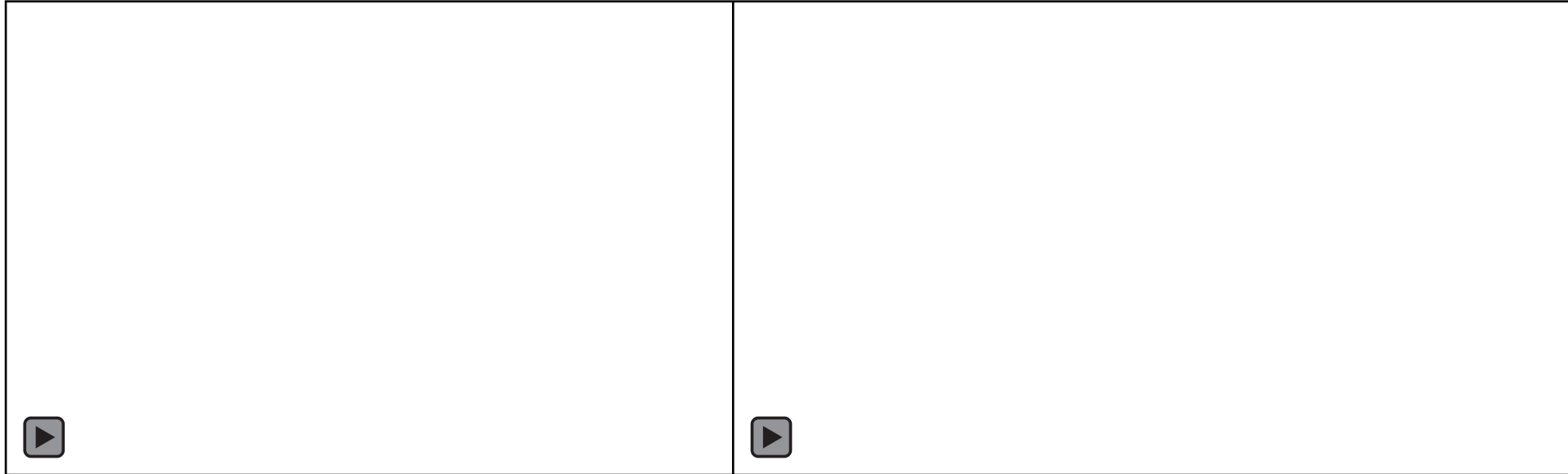


Measured  $V^2/R$  scaling of volume loss vs. HEAF voltage.

# Prior Small Scale Bus Bar Experiments



Evolved metal particle collection and analysis



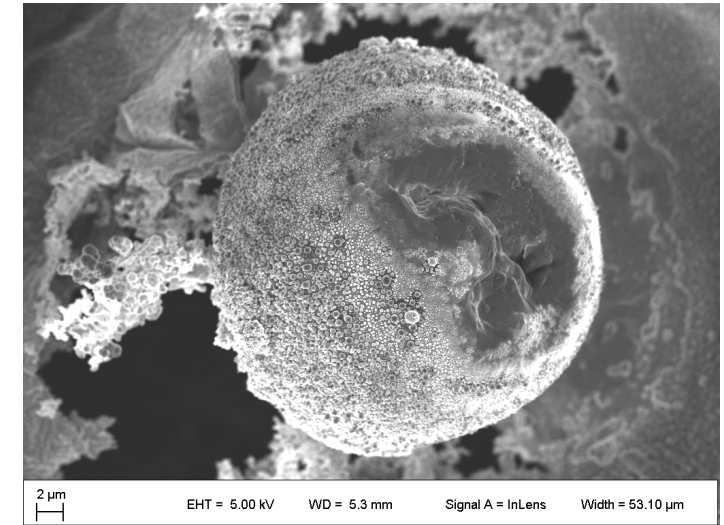
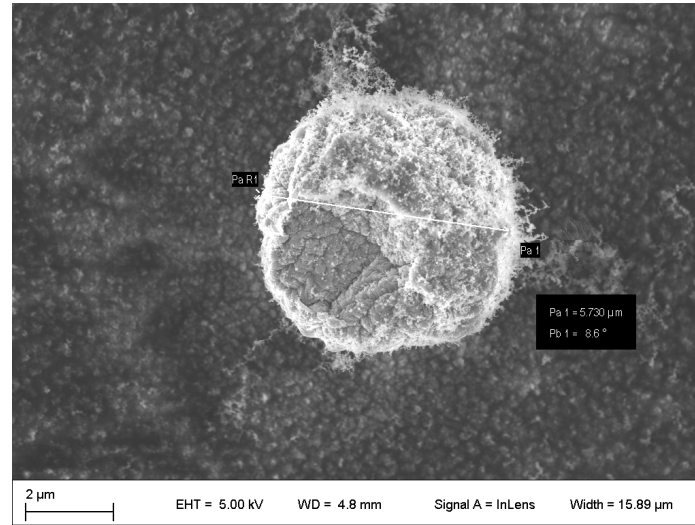
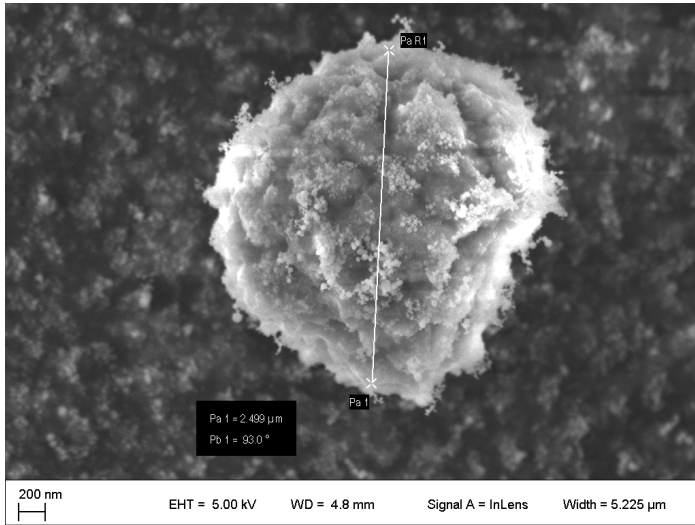
## Key questions:

- 1) quantify evolved aluminum particle size and degree of aluminum oxidation
- 2) correlate aluminum particle oxidation with distance from switchgear
- 3) identify other potential sources of non-electrical incident energy and net energy contribution (heat of oxidation – aluminum, steel and other sources)

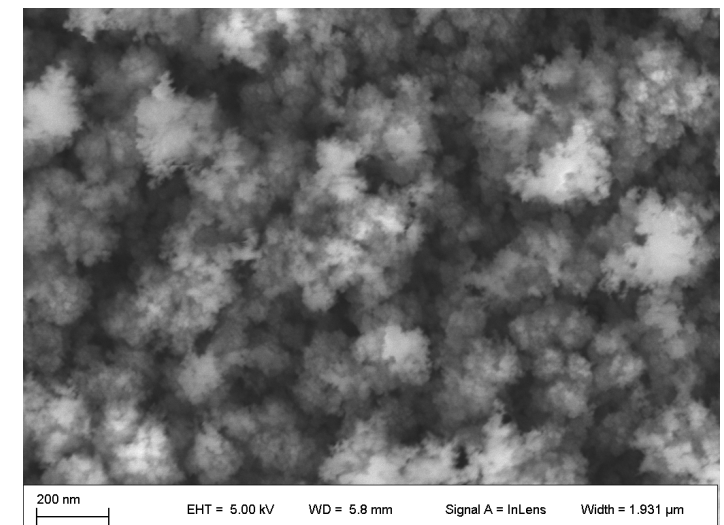
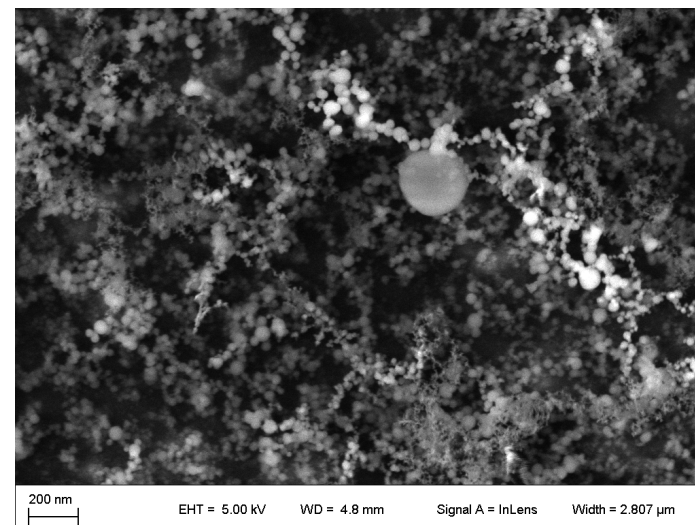
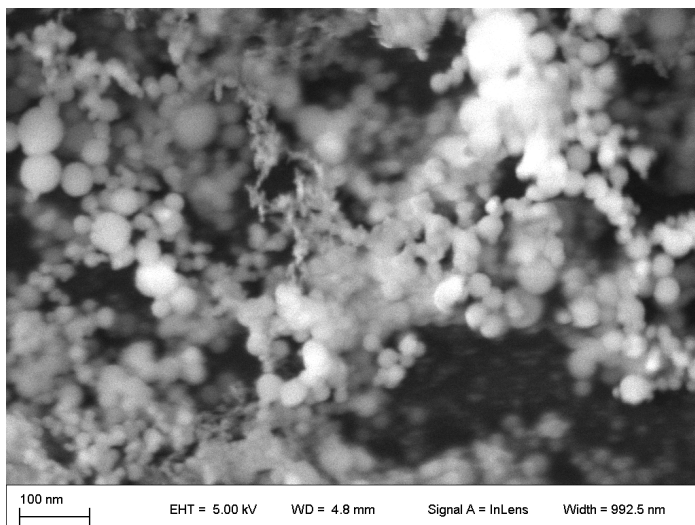
# Particle Collection from 6.9 kV Arc Experiments



6.9 kV arc-generated Al particles (2.5-14  $\mu\text{m}$ ) were collected on aerogel substrates and carbon microscopy tape



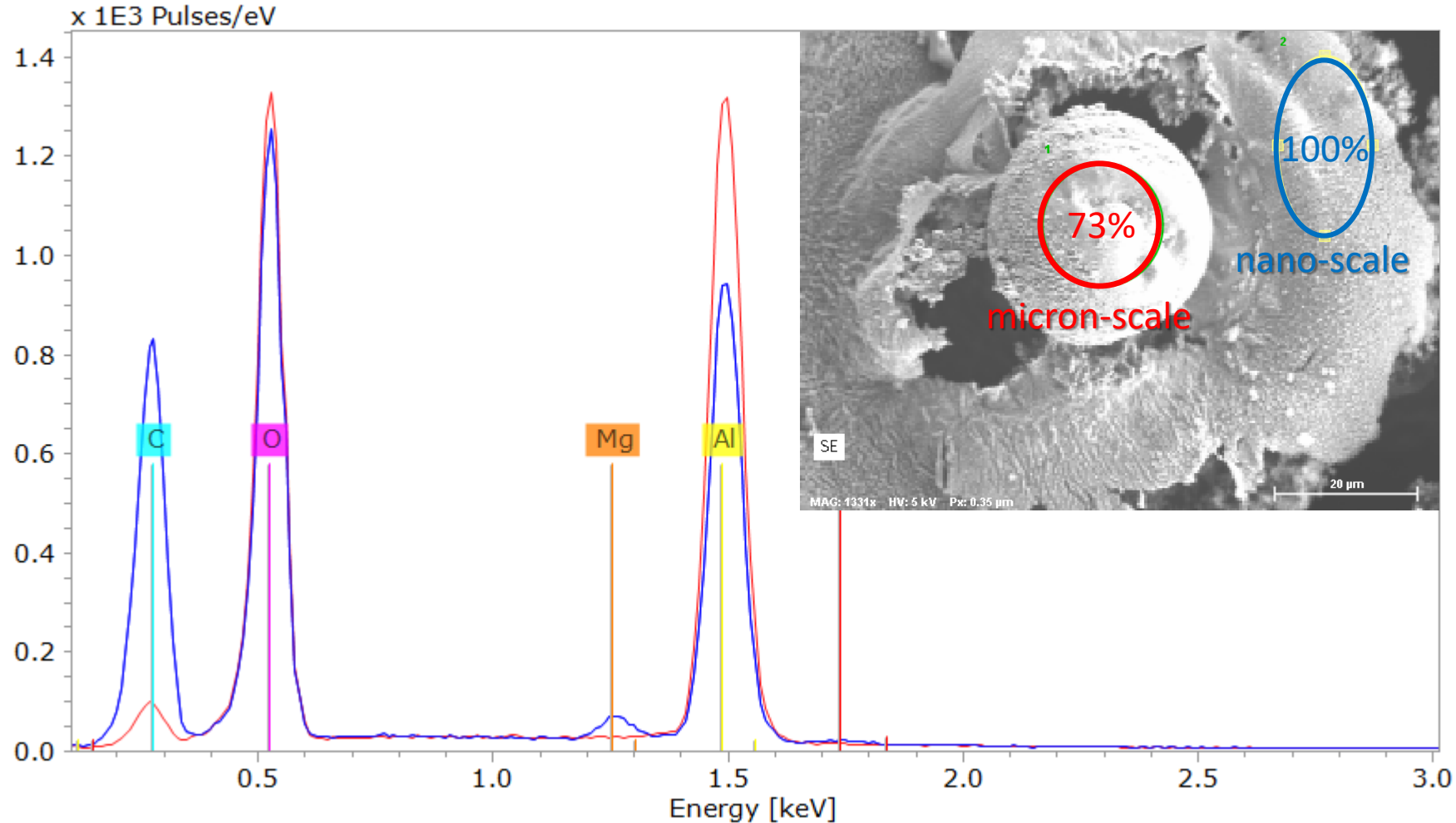
Surfaces of carbon tape and Al particles are coated with nanoparticle (5-30 nm) aluminum oxide particles



# Particle Oxidation Analysis from 6.9 kV Arc Experiments



Degree of oxidation is quantifiable by energy dispersive x-ray analysis (EDS): surface skin vs. full oxidation



Modeling goal: predict quantity of evolved metal and balance of radiated/thermal/oxidative energy evolved

# Multiphysics Arc Modeling Extension



In Aria, a volumetric heat source was pre-defined based upon the modeling results of Lowke [1979] for convectively stabilized arcs, representative of the steady-state heating for arc stabilized predominantly by thermal conduction (see Lowke 1979, Fig. 9).

- Calculations were performed over one-dimension with cylindrical symmetry, representative of arc regions free from the influence of electrode effects. The simulation domain ran from radii of 0 mm to 10 mm, with the outer boundary set to a condition of constant temperature at 273 K (i.e., a thermal wall).
- The resulting temperature profile was checked to ensure a degree of consistency with the pre-defined volumetric heat source. Qualitative agreement with temperature profiles of wall-stabilized arcs (e.g.: Lowke 1979, Fig. 2; Edels 1961, Fig. 10; Kimblin and Lowke 1973, Fig. 4) indicates that the Aria model is on-track and producing physically realistic results. Simple geometries are being modeled June-August 2019.

# ARIA: Governing Equations for Arc Modeling



- Conservation of mass:

$$\frac{\partial \rho}{\partial t} + \underbrace{\nabla \cdot (\rho \mathbf{c}_0)}_{\text{Convection}} = 0$$

- Conservation of momentum:

$$\rho \left[ \underbrace{\frac{\partial \mathbf{c}_0}{\partial t} + \mathbf{c}_0 \cdot \nabla \mathbf{c}_0}_{\text{Advection}} \right] = \underbrace{-\nabla p}_{\text{Hydrostatic pressure}} + \underbrace{\mu \left[ \nabla^2 \mathbf{c}_0 + \frac{1}{3} \nabla (\nabla \cdot \mathbf{c}_0) \right]}_{\text{Viscous pressure}} + \underbrace{\rho \mathbf{g}}_{\text{Buoyancy}} + \underbrace{\mathbf{J} \times \mathbf{B}}_{\text{Magnetic pressure}}$$

- Conservation of energy:

$$\rho c_p \left[ \underbrace{\frac{\partial T}{\partial t} + \mathbf{c}_0 \cdot \nabla T}_{\text{Advection}} \right] = \underbrace{\mathbf{J} \cdot \mathcal{E}}_{\text{Joule heating}} + \underbrace{\lambda \nabla^2 T}_{\text{Diffusion}}$$

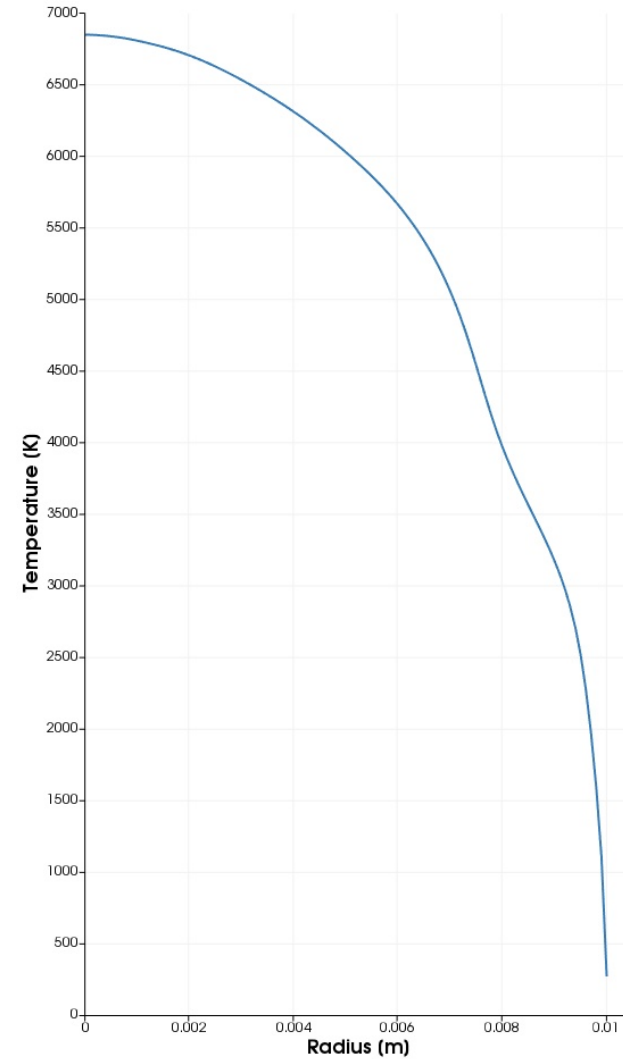
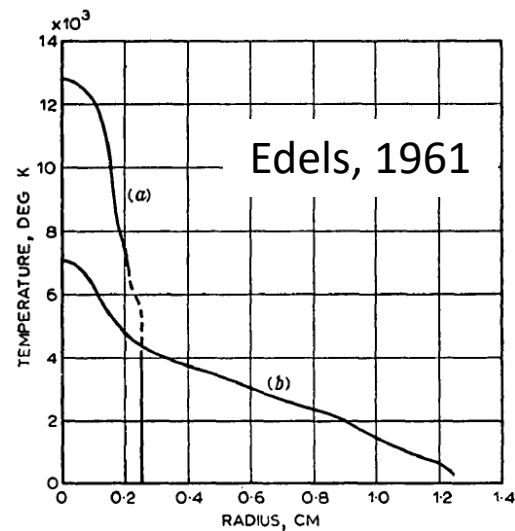
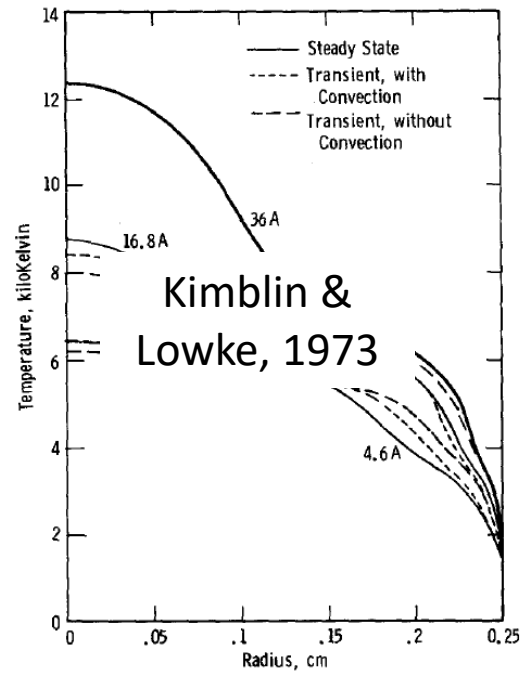
# Progress: Quasi-Transient Arc-Temperature Evolution

## 1-D Radial Analysis



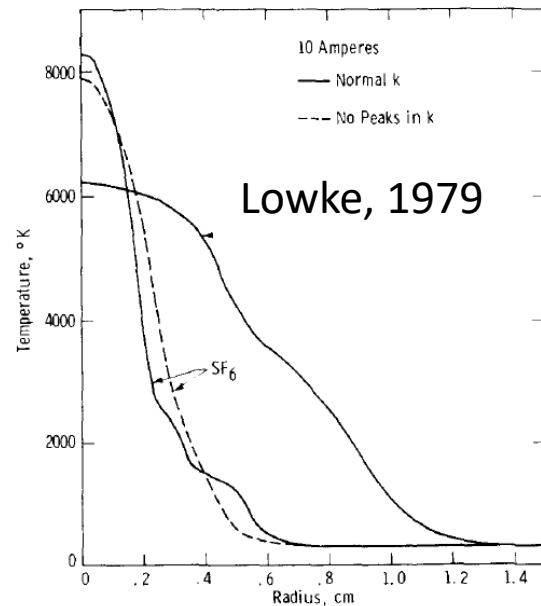
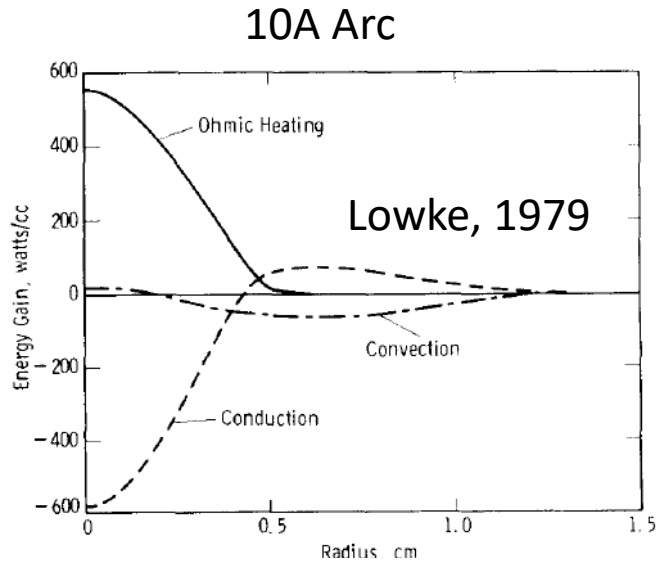
Results of air simulation -- 1D slab, cylindrically symmetric, 10 mm boundary set to 273 K,  
Gaussian input heat profile at 600 W cm<sup>-3</sup> with "1/e" radius of 4 mm

# Arc Modeling Progress

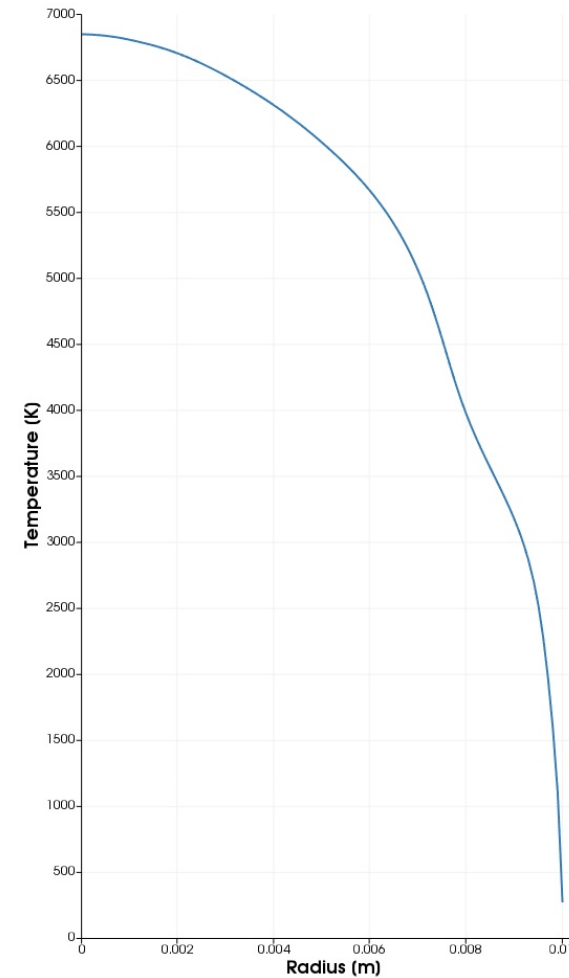


Aria Arc Temperature Model Results

# Arc Modeling Progress



## Aria Temperature Model Results

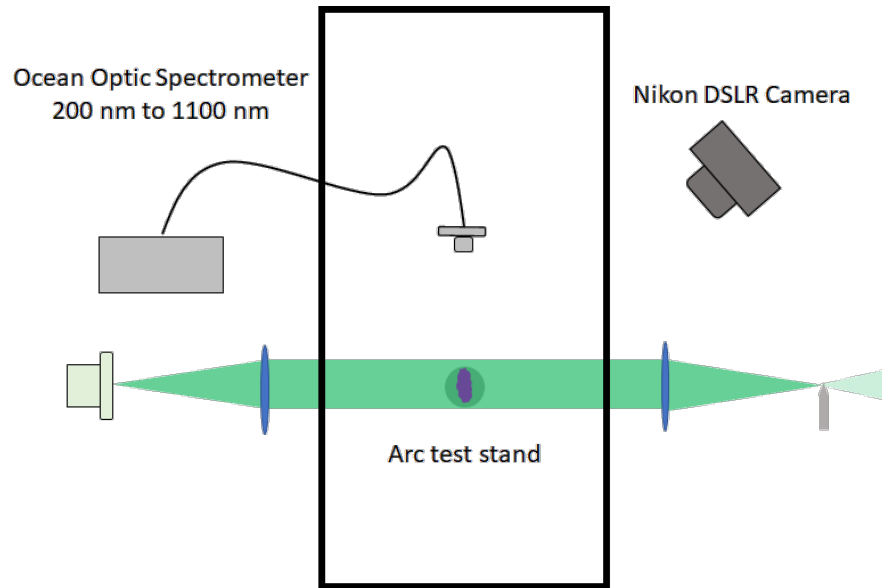


Results of air simulation -- 1D slab, cylindrically symmetric, 10 mm boundary set to 273 K, Gaussian input heat profile at 600 W cm<sup>-3</sup> with "1/e" radius of 4 mm

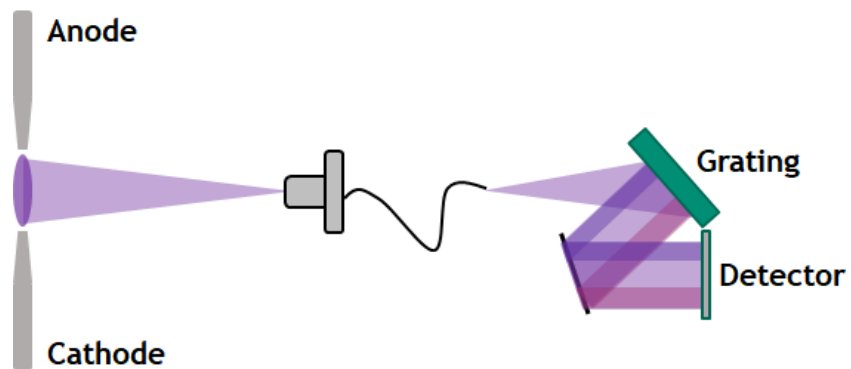
# HEAF Testbed Electrical and Optical Diagnostics



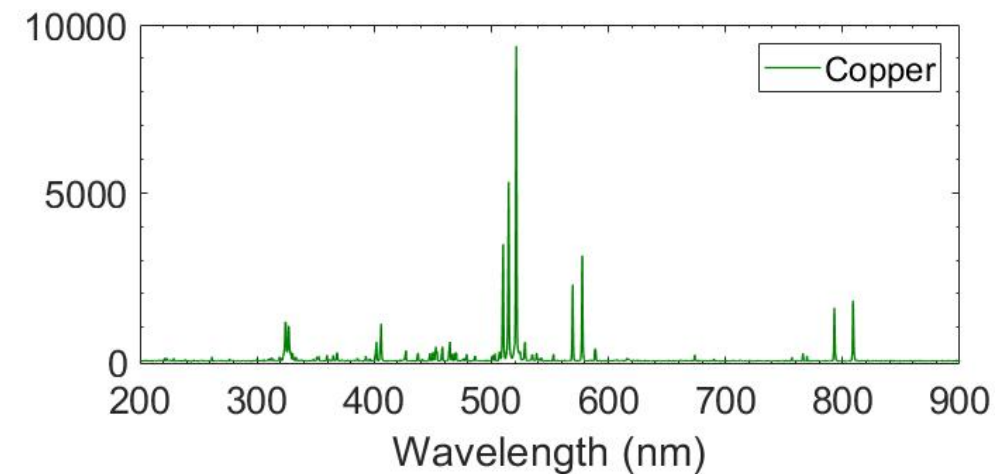
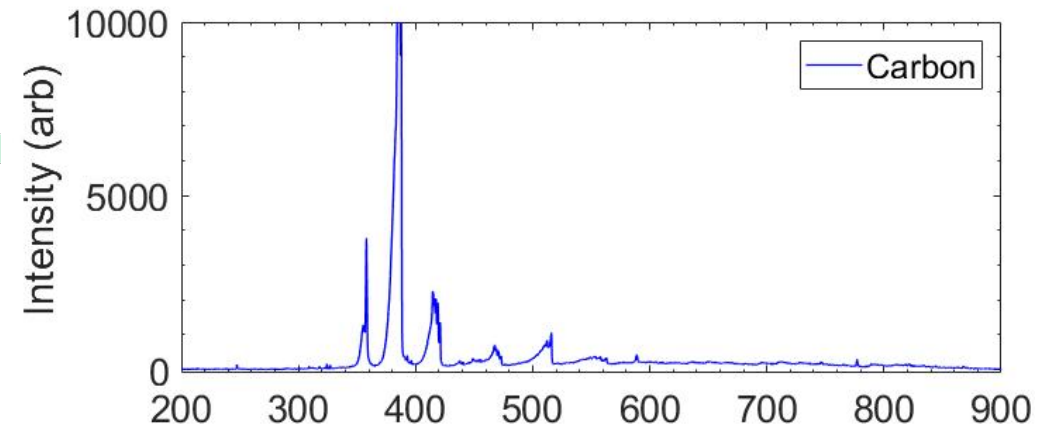
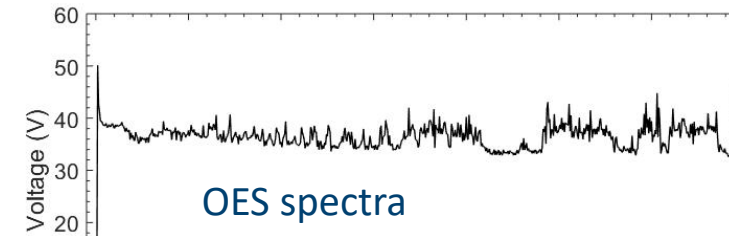
## Experimental Schematic



## Optical emission spectroscopy



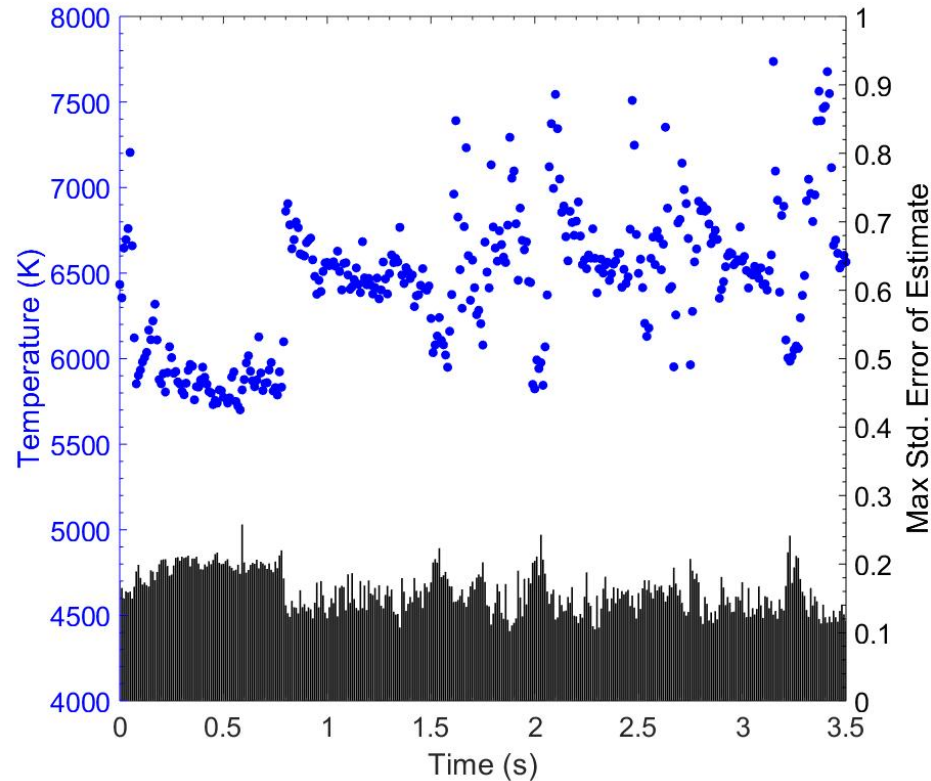
## Traces from DC power supply



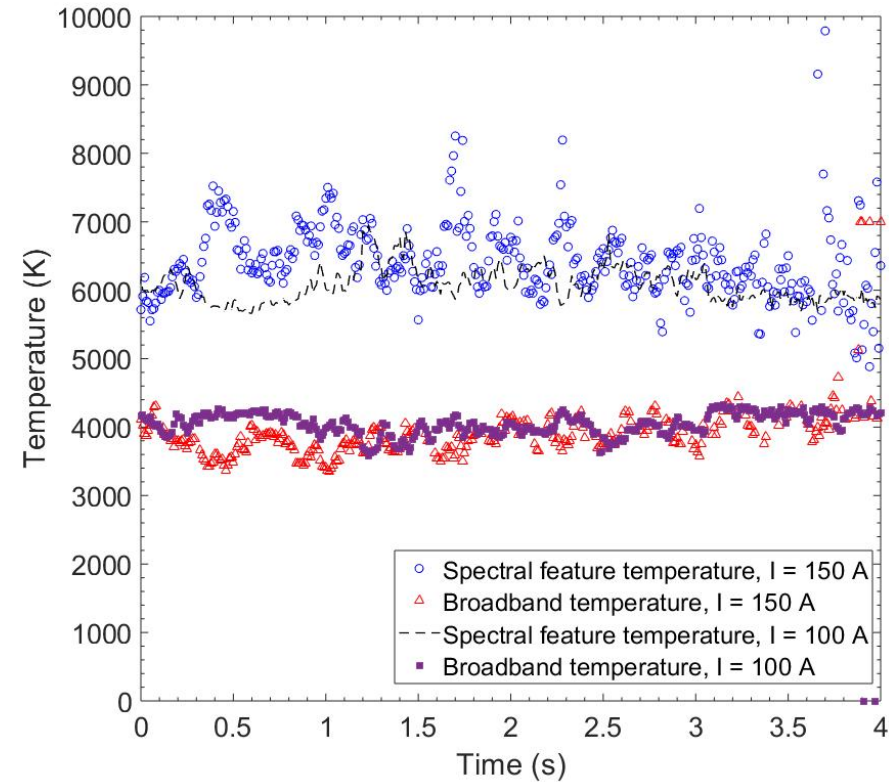
# Spectroscopic Arc Temperature Inference from Cu Vapor



Spectral feature temperatures  
and associated errors



Comparing methods



- Implies temperature inferred from metallic atoms is higher than from broadband emission
- 6000-7000K temperature is in agreement with Aria model 6900K and prior literature (6200-7200K)

# Modeling Next Steps



- Progress towards the next Aria arc-fault simulation benchmark is underway, which will utilize the arc current as an input parameter to replace the pre-defined volumetric heating source.
- This approach requires real-time calculations of the current density to evaluate the evolution of ohmic heating and calculate the temporal physics of arcs in a fully self-consistent way.
- After these developments, we plan to steadily incorporate components of the momentum and mass balance equations to allow for inclusion of convective energy transport, necessary for accurate representation of free burning arcs.
- Beyond this physics, we will include convective energy transport, magnetic forces and the influence of electrode surfaces on the arc
- From this physics-based arc energy “source term”, radiation and conductive heat transport allow:
  - Calculation of volume of electrode melted/vaporized
  - Calculation of equipment breach time (time to  $T_{\text{melt}}$ )
  - Calculation of spatial characterization of temperature field and heat flux

This work will address large gaps in current arc flash studies and improve realism:

- Energy contribution from metal electrodes is ignored
- Enclosure is assumed to be open

# Target Fragility and Failure Criteria

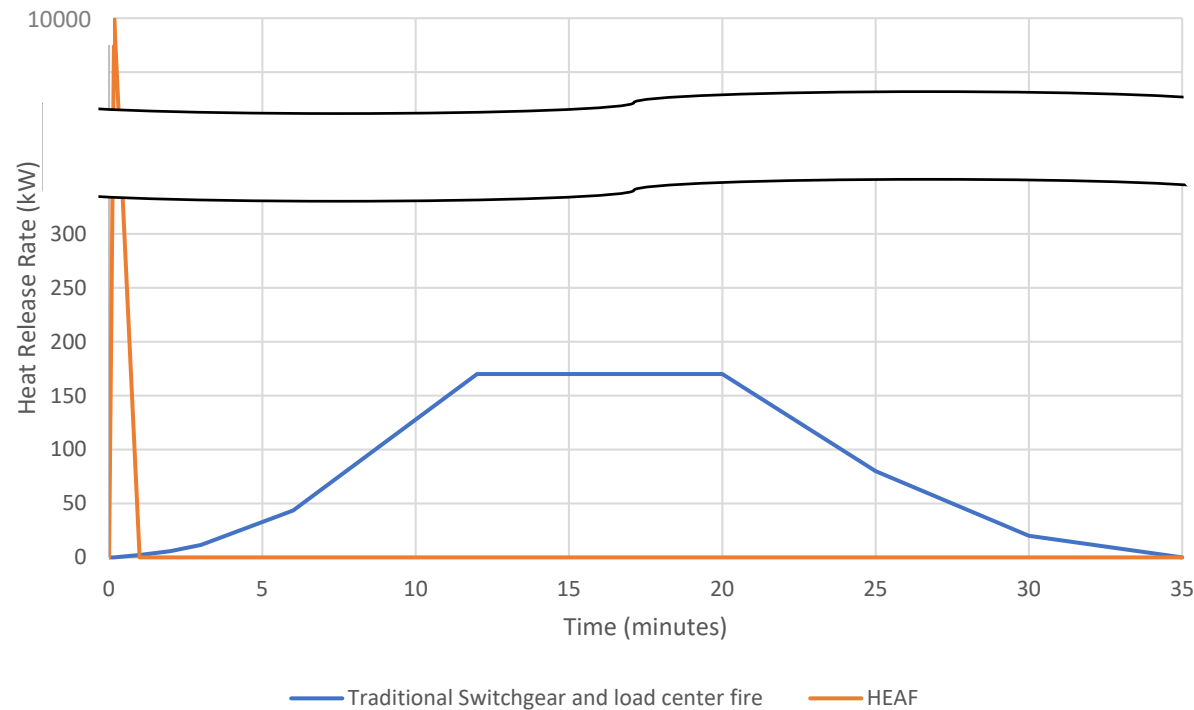


# Failure Criteria



- Failure Criteria is **independent** of energy release prediction/calculation/measurement from HEAF
- Failure Criteria is a characteristic of the target equipment
- Target Equipment list will be developed by the joint NRC/EPRI Working Group

Comparison of Heat Source Term Profile



Target	Temperature/ Time	Incident Energy/time	Breakdown strength
Cables TS			NA
Cables TP			NA
Cable tray			NA
Transformers			
Switch Gear			
Electrical cabinets			

# Cable Failure Criteria



- NUREG/CR-6850 based on typical fire growth HRR of exposing fire
- Cable failure time is when insulation reaches criteria temp
- Thief Model and 6850 Empirical Approach for short duration not sufficient for HEAF durations and energy release

	Radiant Heat	Temperature
TP	6 kW/m <sup>2</sup>	205 C
TS	11 kW/m <sup>2</sup>	330 C

	Exposure Temp	Time to Failure(min)	Heat Flux kW/m <sup>2</sup>	Time to Failure(min)
TS: XLPE Rockbestos Firewall III	>490 C	1	>20	1
TP: PE insulated cables	>370	1	>16	1

- Approach:
  - Predictions for a thermoset and thermoplastic cable will be made for a range of incident energy values to determine range when cable meets critical temperature when exposed for HEAF durations.
  - Confirmatory tests will be conducted measuring under-jacket temperature and monitoring of circuit in parallel cables
  - Incident energy will be provided by most appropriate source to HEAF emitted energy

# Sandia National Labs Model Information



# Sierra Mechanics



- Sierra is an engineering mechanics simulation code suite supporting the Nation's Nuclear Weapons mission as well as other customers
- Multiple codes based on a common foundation of mesh generation, input syntax, parallel processing, and communication utilities
  - Solid mechanics: Implicit quasi-statics, implicit dynamics, explicit dynamics
  - Structural dynamics
  - Thermal/fluid:
    - Aria: Thermal, incompressible fluid dynamics, multiphysics
    - Fuego: Reacting low-Mach fluid dynamics
    - Aero: Compressible, high-Mach fluid dynamics
    - Nalu: Low-Mach fluid dynamics, open-source
  - Cubit: Mesh generation
  - Paraview: Simulation visualization
- Coupling between Sierra codes and to select other codes (CTH, etc).

# Sierra/Multiphysics: Aria



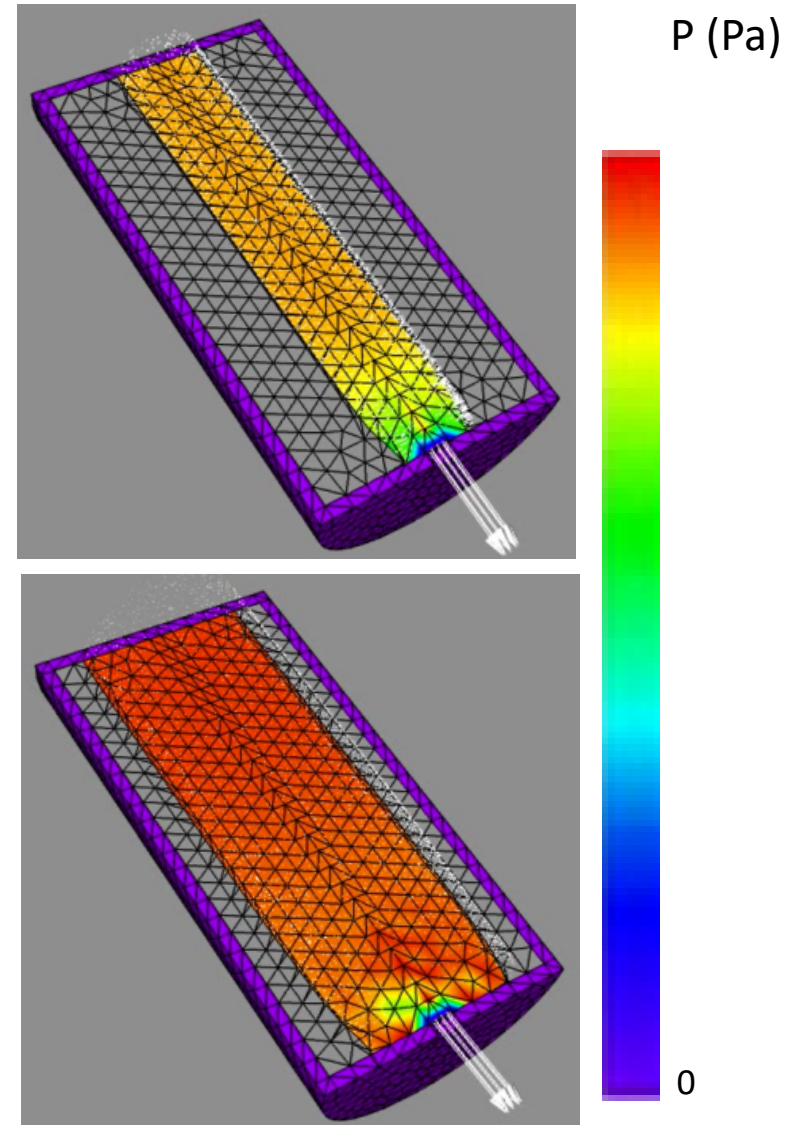
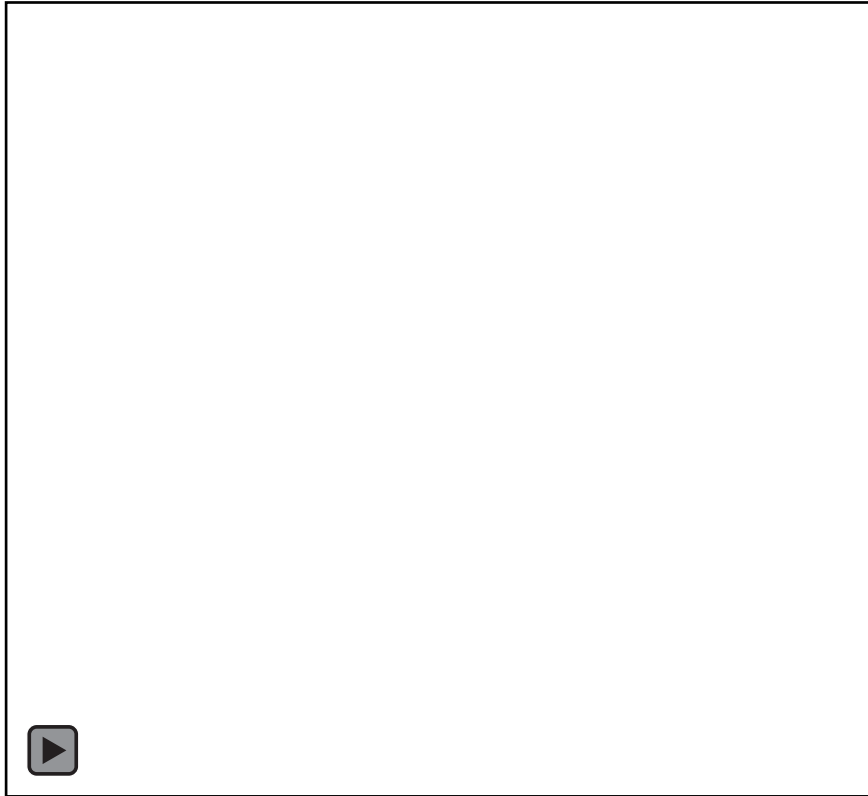
- Aria is a multi-physics, finite-element method code
  - Origins are GOMA, which was created for manufacturing (welding, coating, etc.).
- Fully parallel with MPI, scales to 1000s of cores
- Full-Newton nonlinear solution scheme
- Variety of direct and iterative linear solvers (Trilinos)
- Solved a variety of equations with varied couplings
  - Conservation of energy, mass, momentum (fluid), momentum (solid)
  - Species transport, generalized chemistry, voltage, current
  - Level-set, radiation transport, porous flow, lubrication, etc.
- Traditionally FEM with P0, Q1, Q2 basis functions.
- Monolithic & loose couplings (equation systems, solution control)
- Coupled to many other Sierra codes (Adagio, Fuego, Cantera)

# Aria: Conductive burn of energetic materials



## Physics

- Reaction chemistry
- Interface physics
- Compressible gases
- Solid mechanics

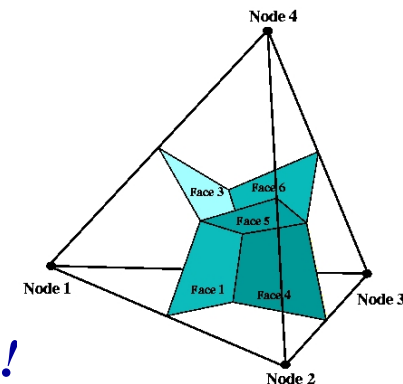
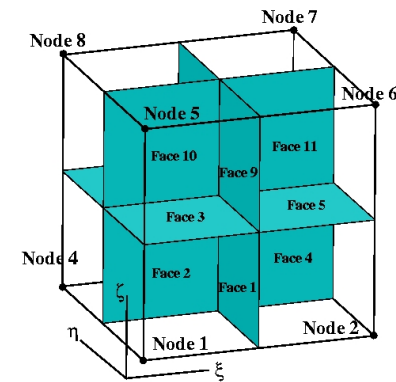


# SIERRA/Fuego/Syrinx/Calore Methodology and Framework



- Common application framework
  - Shared data structure, parser, file I/O, parallel communication, solvers, etc.
- Data exchange for application coupling

- **SIERRA/Fuego**: Low-Mach turbulent fire
  - Hybrid control volume finite element method (CVFEM)
- **SIERRA/Syrinx**: Participating media radiation (PMR)
  - Streamwise-upwind Petrov-Galerkin FEM
- **SIERRA/Calore**: Heat conduction, enclosure radiation
  - Galerkin FEM



*Each code has completed a detailed verification suite!*

# Fluids Numerical Overview CVFEM



- Backward Euler or Crank-Nicholson time solution
- Equal-order interpolation CVFEM technique for low-Mach and moderately acoustically compressible mechanics
  - Approximate pressure projection method for continuity/momentum
  - Generalized Newton solve (full analytical sensitivities) with pressure stabilization
- Convection operators: Central, pure upwind, skew upwind, MUSCL w/flux limiters, SUCV

Continuity:  $\int \frac{\partial \bar{\rho}}{\partial t} dV + \int \bar{\rho} \tilde{u}_j n_j dS = 0$

Momentum:  $\int \frac{\partial \bar{\rho} \tilde{u}_i}{\partial t} dV + \int (\bar{\rho} \tilde{u}_i \tilde{u}_j n_j + \bar{p} n_j \delta_{ij}) dS = \int (\bar{\tau}_{ij} - \tau_{u_i u_j}) n_j dS + \int (\bar{\rho} - \rho_o) g_i dV$

Enthalpy:  $\int \frac{\partial \bar{\rho} \tilde{h}}{\partial t} dV + \int \bar{\rho} \tilde{h} \tilde{u}_j n_j dS = - \int (\bar{q}_j + \tau_{hu_j}) n_j dS - \int \frac{\partial \bar{q}_i^r}{\partial x_i} dV + \int \left( \frac{\partial P}{\partial t} + \tilde{u}_j \frac{\partial P}{\partial x_j} \right) dV + \int \tau_{ij} \frac{\partial u_i}{\partial x_j} dV$

Species:  $\int \frac{\partial \bar{\rho} \tilde{Y}_k}{\partial t} dV + \int \bar{\rho} \tilde{Y}_k \tilde{u}_j n_j dS = \int (\bar{\rho} \tilde{Y}_k \hat{u}_{j,k} - \tau_{Y_k u_j}) n_j dS + \int \tilde{\omega}_k dV$

Turbulence closure models required

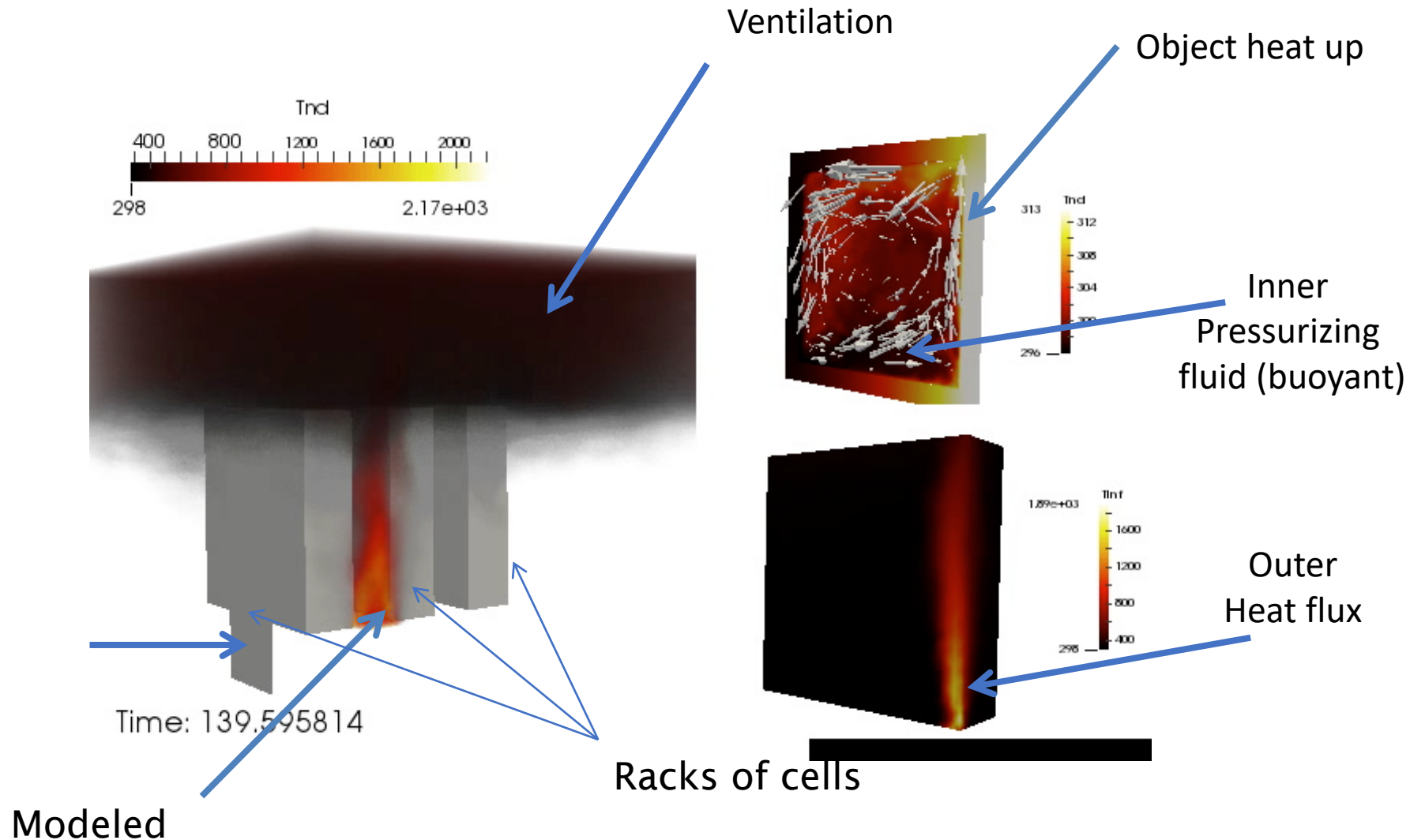
Chemistry and subgrid mixing model



# Prior Aria/Fuego coupling: Battery Safety Large-scale Storage Facilities



# Applying Sierra Simulation Tool to Battery Fire Scenarios



# Ventilation Effect on Fire Plume Dynamics (0 m/s)



# Ventilation Effect on Fire Plume Dynamics (10 m/s)



# Questions

